OPTIMIZATION OF BUCKLING BEHAVIOR OF HYBRID COMPOSITE BEAM UNDER AXIAL COMPRESSION

A Thesis Submitted to
the Graduate School of Engineering and Sciences of
İzmir Institute of Technology
in Partial Fulfillment of the Requirements for the Degree of

MASTER OF SCIENCE

In Mechanical Engineering

by
Hayri ALTINTAŞ

December 2021
İZMİR

To My Parents…

ACKNOWLEDGMENTS

I would like to express my endless thanks to my academic supervisor Prof. Dr. H. Seçil Artem for her continuous support, patience, motivation, and valuable advice. I will always be proud to work with Prof. Artem throughout my thesis study.

I would like to thank Assoc. Prof. Dr. Levent Aydın, Asst. Prof. Dr. Arda Deveci, who are members of the Optimization Modeling and Applied Math Research Group (OMA-RG).

I should state that I am grateful to my family who has always encouraged me along this way. I would also like to thank my sister Gizem Altıntaş for her support. Furthermore, I offer sincere thanks to my girlfriend Aybüke Güzel, she has always supported me in this difficult journey.

Lastly, I would like to thank the people who helped me directly and indirectly.

ABSTRACT

OPTIMIZATION OF BUCKLING BEHAVIOR OF HYBRID COMPOSITE BEAM UNDER AXIAL COMPRESSION

The use of lighter and high-performance materials in the aerospace sector is of great importance. Optimization methods, which have become very popular with the technological development in the production methods of composite structures in recent years and provide the most suitable design for the purpose, are frequently preferred in the design of parts in the aviation industry. Determining the buckling load capacity of a composite beam under compression load is very important for the design of composite structures.

The buckling load capacity of a hybrid composite beam with fiber metal laminate (FML), which is frequently used between aircraft wing and fuselage. The optimum design of the anti-buckling behavior of the hybrid composite beam, which is subjected to compression load, fixed by simple support on both sides, was performed by a genetic algorithm (GA) based on the Tsai-Wu fracture criterion. The robust design of composite hybrid laminates was developed using a design optimization process based on GA with the finite element method. A multi-objective genetic algorithm (MOGA) was used to optimize the design of a hybrid composite beam subjected to buckling. Design variables in the optimization process are considered as fiber material and angle orientations. The purpose of the objective function is to reduce the equivalent stress of hybrid composites while increasing critical buckling load. The design constraint was the Tsai-Wu failure index.

As a result, it has been observed that the buckling performance of the beam depends on the structure of the metal material in FML composites. Carbon/epoxy and glass/epoxy structures were proposed and a design was aimed according to the maximum buckling load in the best stacking sequence, taking into account the data in the design constraints.

Keywords: *Buckling, Fibre Metal Laminate, Thin-Walled, Genetic Algorithms, Hybrid Composite, Tsai-Wu Failure Criterion, Finite Element Analysis.*

ÖZET

EKSENEL BASMA ALTINDAKİ HİBRİT KOMPOZİT KİRİŞİN BURKULMA DAVRANIŞININ OPTİMİZASYONU

Havacılık ve uzay sektöründe daha hafif ve yüksek performanslı malzemelerin kullanılması oldukça büyük önem taşımaktadır. Özellikle son yıllarda kompozit yapıların üretim yöntemlerindeki teknolojik gelişim ile oldukça popüler hale gelmiş olan ve amaca en uygun tasarım elde etmeyi sağlayan optimizasyon yöntemleri, havacılık sektöründe parça tasarımında sıklıkla tercih edilmektedir. Bası yükü altındaki bir kompozit kirişin burkulma yükü kapasitesinin belirlenmesi kompozit yapıların tasarımı için çok önemlidir.

Uçak kanat ve gövde arasında sıklıkla kullanılan fiber metal laminatlı (FML) bir hibrit kompozit kirişin burkulma yükü kapasitesi incelenmiştir. İki tarafından da basit mesnetle sabitlenmiş basma yüküne maruz kalan hibrid kompozit kirişin burkulma karşıtı davranışlarının optimum tasarımı Tsai-Wu kırılma kriteri esas alınarak genetik algoritma (GA) ile gerçekleştirilmiştir. Kompozit hibrit laminatların sağlam tasarımı, GA ve sonlu elemanlar yöntemine dayalı bir tasarım optimizasyon süreci kullanılarak geliştirildi. Burkulmaya maruz kalan hibrit bir kompozit kirişin tasarımını optimize etmek için çok amaçlı bir evrimsel algoritma (MOGA) kullanıldı. Optimizasyon prosesindeki tasarım değişkenleri, fiber malzemesi ve açı yönelimleridir. Amaç fonksiyonunun amacı, kiriş kritik burkulma yükünü arttırırken hibrit kompozitin eşdeğer stresini azaltmaktır. Tasarım kısıtı ise Tsai-Wu kırılma indeksidir.

Sonuç olarak, kirişin burkulma performansı FML kompozitlerde metal malzemenin yapısına bağlı olduğu gözlemlenmiştir. Karbon/epoksi ve cam/epoksi yapı önerilerek tasarım kısıtlarındaki veriler göz önüne alınarak en iyi açı yönlerinde maksimum burkulma kuvvetine göre tasarım önerilmiştir.

Anahtar Kelimeler: *Burkulma, Fibre Metal Lamine, İnce Duvarlı, Genetik Algoritma, Hibrit Kompozit, Tsai-Wu Hasar Kriteri, Sonlu Elemanlar Analizi.*

TABLE OF CONTENTS

LIST OF FIGURES

Figure **Page**

Figure **Page**

LIST OF TABLES

Table **Page**

CHAPTER 1

INTRODUCTION

1.1. Literature Survey

Due to its distinct advantages over metal counterparts such as higher specific strength/stiffness ratio, superior corrosion and fatigue resistance, fiber reinforced laminated composites have been used in many technical applications such as aircrafts, aerospace, automotive, and marine industry. Lightweight, strong, and stiff airplane frames, composite drive shafts and suspension components, sports equipment, pressure containers, and high-speed flywheels with developed energy storage capacities are some of their applications.

The anisotropic nature of fiber-reinforced composites allows for the one-of-a-kind ability to modify features like stacking sequence, fiber orientation, and laminate thickness to meet design requirements for a specific application. As a result, multiple objective functions and design factors can be used to optimize the design of laminated composite materials (Pelletier and Vel 2006).

In the design phase of laminated composites, optimization has become critical. Customizing fiber angle, ply thickness, number, and material (hybridization) to accomplish the appropriate criteria for varied loading circumstances can improve the structural performance of composite laminates. As a result, several studies have been conducted to determine the best design for laminated composites. Fiber orientation angles and layer thickness were considered design variables in the majority of these investigations. Different optimization approaches, such as the genetic algorithm (GA), gradient based optimization (GBM), and particle swarm optimization (PSO), were used to optimize various objective functions (Beylergil 2020).

One of the design aims employed by researchers is to reduce the weight or thickness of laminated composite beams. Some pioneers are investigating the use of a genetic algorithm for the least thickness design of composite laminated beams. A genetic method for laminate design that had previously been created has been refined and improved. As a result, the thinnest symmetric and balanced laminates satisfying the 4-ply contiguity

constraint are constructed, which do not fail due to buckling or excessive strains (Le Riche and Haftka 1995). For different in-plane loading conditions and different ply orientations, which are defined as the design variable, a minimum weight design of composite laminates is presented using a genetic algorithm that considers failure mechanism based, maximum stress, and Tsai-Wu failure criteria as design constraints (Naik, et al. 2008).

Minimum weight design has been combined with minimum deflection or minimum cost design aims by several researchers. The minimum deflection and weight designs of laminated composite plates with four layers are given separately using the finite element method based on Mindlin plate theory in conjunction with optimization routines, taking into account various boundary conditions, varying aspect ratios, and different loading types (Walker 1997). A technique for combining GA with the finite element method to minimize both the mass and deflection of eight layered symmetric-balanced fiber-reinforced composite plates with fiber orientation and laminate thickness design variables is described in a similar study, using the Tsai-Wu failure criterion as the implemented design constraint (Walker and Smith 2003). A genetic algorithm is used to determine the minimal weight and material cost of laminated plates subjected to in-plane loads. Maximum stress, Tsai-Wu, and the Puck failure criteria are all taken into account by the optimization problem's constraints. The ply orientations, the number of layers, and the layer material, as usual, are the design factors (Lopez, et al. 2009).

For the design of composite structures, the buckling load capacity of a composite plate under in-plane compressive loads is critical. The buckling could lead to the structure's early failure. As a result, buckling load maximization is a crucial problem that many researchers are working on. Haftka and Le Riche (1993) used a genetic algorithm to study the stacking sequence design of a composite laminate for buckling load maximization while considering strain failure. Using a GA and a generalized pattern search technique, the best stacking sequence designs for a composite panel subjected to biaxial in-plane compressive stresses were discovered. In their work, the critical buckling loads are maximized for a variety of load cases and plate aspect ratios, and the findings are compared to published data (Soykasap and Karakaya, 2007 and 2009).

Another optimization study employing a genetic algorithm is proposed to determine the optimal stacking sequence of laminated composite plates for the maximum buckling load under a variety of loading conditions, including uniaxial compression, shear, biaxial compression, and a combination of shear and biaxial loadings. Fiber orientations are used

as design variables and the critical buckling load is used as a fitness function (Kim and Lee 2005).

Some academics have enhanced and changed genetic algorithms for finding the best composite plate designs and generating more trustworthy results. The application of a genetic algorithm with generalized elitist election to the buckling load maximization of a simply supported laminated composite plate has been investigated in order to produce optimal designs for symmetric-balanced, simply supported plate assumptions (Soremekun, et al. 2001). Liu et al. have developed permutation genetic algorithms for optimizing the stacking sequence of a composite laminate for maximum buckling stress and a comparison with normal non-permutation GA (Liu 2000).

Buckling load maximization designs, like weight minimization design challenges, have been addressed in the literature using a variety of optimization approaches. Erdal and Sonmez used an improved version of the simulated annealing algorithm, called direct simulated annealing, to optimize the buckling load capacity of laminated composites subjected to given in-plane static stresses for critical buckling failure in order to discover the best fiber orientation (Erdal and Sonmez 2005). Using a heuristic search technique known as tabu search, optimal designs of the stacking sequence of a composite laminate for buckling response, matrix cracking, and strength requirements have been completed and compared to comparable earlier studies done by GA (Pai, et al. 2003). The buckling load is optimized under worst case in-plane loading using a nested solution method, and the optimal design of composite laminates under buckling load uncertainty is examined. Using a nested solution method, results are given for both continuous and discrete fiber orientations (Adali, et al. 2003). Under three hundred load situations, a Pareto-based multi-objective evolutionary algorithm method is used to optimize the design of a composite plate for weight minimization and maximizing of buckling margins (Irisarri, et al. 2009).

Deveci and Artem used the Failure Tensor Polynomial in Fatigue in order to fatigue life prediction model to optimize the stacking sequence of laminated composites for better fatigue life under varied in-plane cyclic loadings. They employed a hybrid method (a mix of genetic and extended pattern search algorithms) to find the optimal discrete fiber angles for the longest fatigue life (Deveci et al. 2016).

Temperature buckling optimization of composite laminates subjected to a thermal change has been researched in the literature, in addition to buckling load optimization of composite plates subjected to mechanical stress simply. Spallino and Thierauf use

evolution strategies, a guided random-search method, to solve the thermal buckling optimization problem of laminated composite plates in aerospace structures, which require such components that can withstand external environment loads without loss of stability, subject to a temperature rise (2000). Another study uses the Modified Feasible Direction Methods approach to analyze thermal buckling optimization of laminated plates subjected to evenly distributed temperature load in order to find optimum fiber orientation designs with the largest critical temperature capacity of laminated plates (Topal and Uzman 2008).

This study the buckling and post-buckling behavior of thin-walled Fibre Metal Laminate (FML) profiles subjected to axial loading. The research focuses on open cross-section profiles made up of alternating thin aluminum layers and fibre-reinforced unidirectional prepreg. The autoclaving process was used to create the laboratory tested specimens. Various 3/2-layer stackings were investigated and subjected to axial compression in buckling experiments depending on fibre alignment. The results of extensive experimental research were compared to FML panel/column modeling in FEA and analytically investigated using Koiter's asymptotic theory (Banat et. al.2016).

A multiobjective evolutionary algorithm was used to optimize the design of a hybrid composite laminate that was exposed to eccentric loading (MOGA). Design variables included the ply material and fiber orientations. The goal of the objective function was to reduce cost and weight while increasing rigidity. The maximum Tsai-Wu failure index and first mode natural frequency were the design limitations (Beylergil 2020).

For the plane wing, control buckling behavior in structural parts of a composite wing for future morphing application to provide unique tailorable and effective methods. Rather than fighting buckling with traditional design, the concept is to welcome it by leveraging the nonlinear post-buckling response to regulate stiffness changes that redistribute the load in the wing structure. The suggested procedures allow for successful multi-stable configuration design and illustrate the ability to achieve composite wing morphing using controlled buckling behaviors in structural components (Zhang 2021).

1.2. Objectives of the Study

The development of hybrid composite/metal materials for aerospace applications in recent decades has created an innovative family of materials known as Fibre Metal Laminates (FMLs), which are made up of alternating thin metal layers and layers of a fibre-reinforced composite material see Fig. 1.1.

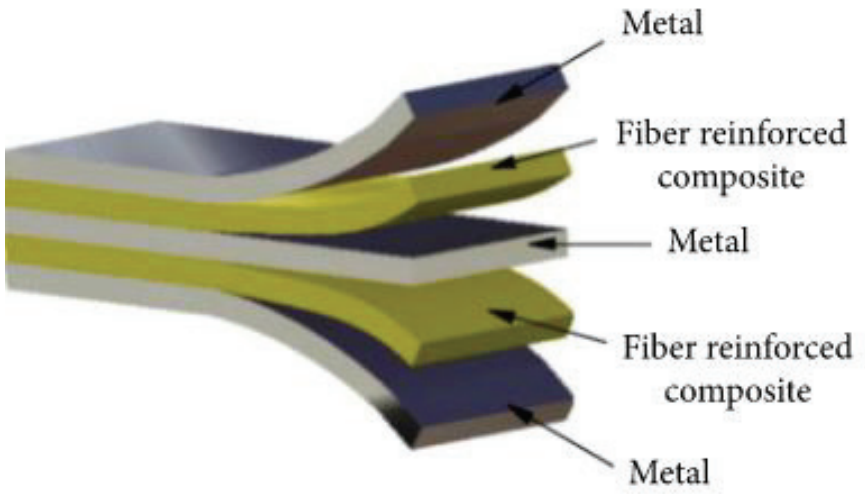

Figure 1.1. Fibre-reinforced composite and metal layers composition of fibre metal laminates. (Source: Chen et. al. 2020)

FMLs are a type of composite that is made by combining fibre-reinforced laminates with metallic layers. Moreover, the majority of FML applications are now based on u unidirectional glass fibre-reinforced prepregs paired with aluminum alloys sheets (Soltani et. al. 2011).

Lighter, more flexible constructions will be required for next-generation aircraft, with the same or higher levels of safety. With the developments in production methods, the use of carbon fiber and glass fiber derivative composite materials has increased by using filament winding methods for cheaper (Zhang 2021).

Based on the literature review, it is clear that design requirements include spar beam performance, material failure, weight, rigidity, and so on, in order to optimize the number of plies (thickness) and stacking sequences for a better design. In this context, the aim of the thesis can be listed as follows:

1) Investigated the buckling behavior for the channel section FML beam was with the Finite Element Method (FEM). Aimed to reach the best fiber angle of the existing FML with GA optimization.
2) To investigate the optimum design of composite hybrid laminates (carbon/epoxy, glass/epoxy) with channel section (C-shaped) subjected to compressive load.
3) Determination of the best stacking sequences for C-shaped hybrid composite beam (carbon/epoxy, glass/epoxy) using a Multi-Objective Evolutionary Algorithm (MOGA).
4) Determination and comparison of the critical buckling load, maxsimum equivalent stress, and the Tsai - Wu failure criteria of the optimized composite beam for the design condition.

CHAPTER 2

COMPOSITE MATERIALS

2.1. Introduction

Materials have such a significant impact on our lives that they have ruled and been named after historical periods throughout human history. Composites, plastics, and ceramics have dominated new materials for the past four decades. Composite materials have constantly increased in volume and number of applications, continuously pushing into and gaining new sectors (Barbero 2010).

A composite is a structural material made up of two or more components that are macroscopically combined but are not soluble for each other. One of the components is known as the reinforcement, and the one in which it is embedded is known as the matrix. The reinforcement material could be fibers, particles, or flakes. The matrix materials are typically continuous. Composite systems include concrete reinforced with steel and epoxy reinforced with glass fibers, carbon fibers, etc. among many other items (Kaw 2006).

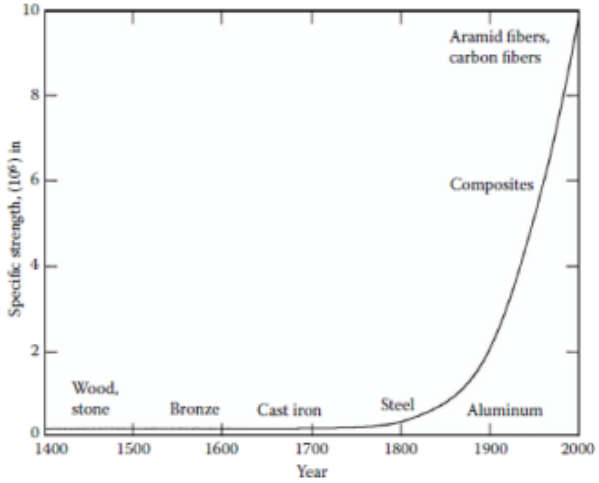

Figure 2.1. Specific strength of materials as a function of period of usage (Source: Kaw 2006)

When compared to many traditional metallic materials, many fiber-reinforced materials provide a better combination of strength and modulus. These composite materials outperform metallic materials due to their low density, high strength-weight and modulus-weight ratios. Moreover, many laminated composites have good fatigue strength and fatigue damage tolerance. As a result, fiber reinforced materials have emerged as a significant class of structural materials, and they are being considered for use as metal substitutes in many weight-critical components in aerospace, automotive, and other industries (Mallick 2007).

2.2. Classification of Composite Materials

Composite material is presented in the form of common fiber and matrix types, which are then assembled into composites. Many different types of reinforcement, mostly fibers, are commercially available. Their properties are determined by atomic structure and the presence of defects, both of which must be controlled during manufacturing. Polymers, metals, and ceramics can all be used to create matrices. The matrix is usually chosen based on the required properties, component geometry, and manufacturing method (Cylne 2019).

2.2.1. Matrix Composite Materials

In composite materials, matrix serves three basic functions. These are used to keep the fibers together, distribute load on the fibers, and protect the fibers from external factors. An optimum matrix material should have a low viscosity structure at first and then easily transition to a solid form capable of enclosing the fibers in a strong and convenient manner (Cylne 2019).

Matrix	Density ρ (kg m^{-3})	Young's modulus E (GPa)	Shear modulus G (GPa)	Poisson ratio ν	Tensile strength σ_m (GPa)	Thermal expansivity α ($\mu\varepsilon$ K^{-1})
Epoxy	1250	3.5	1.27	0.38	0.04	58
Polyester	1380	3.0	1.1	0.37	0.04	150
Polyether ether ketone (PEEK)	1300	4	1.4	0.37	0.07	45
Polycarbonate	1150	2.4	0.9	0.33	0.06	70
Polyurethane rubber	1200	0.01	0.003	0.46	0.02	200
Aluminium	2710	70	26	0.33	0.1–0.3	24
Magnesium	1740	45	7.5	0.33	0.1–0.2	26
Titanium	4510	115	44	0.33	0.4–1.0	10
Borosilicate glass	2230	64	28	0.21	0.05	3.2

Figure 2.2. Giving of properties of several different types of matrix (Source: Clyne 2006)

There are four main types of composites based on the type of matrix they employ polymer matrix composites(PMC), ceramic matrix composites(CMC), metal matrix composites(MMC) and carbon - carbon composites(C/C).

2.2.1.1. Metal Matrix Composite Materials

Metal matrix composites(MMC) have largely been developed using three metals: aluminum, magnesium, and titanium. Metals are usually alloyed with other elements to improve their physical and mechanical properties, and there is a wide variety of alloy compositions available. Thermal and mechanical treatments, which determine the microstructure, have a strong influence on the final properties (Cylne 2019). Figure 2.2 shows some typical properties of common metal matrices.

Metals used in composites are typically ductile and isotropic. In contrast to polymers, the stiffness increases achieved by the incorporation of the reinforcement are frequently small. However, significant improvements in properties such as wear characteristics, creep performance, and thermal distortion resistance are frequently achieved. All three metals are highly reactive and have a high affinity for oxygen. This has implications for composites production, particularly in terms of chemical reactions at the interface between the matrix and the reinforcement, which have proven particularly difficult for titanium (Cylne 2019).

2.2.1.2. Polymer Matrix Composite Materials

Polymer matrix composites (PMCs) are common advanced composites composed of a polymer such as epoxy, polyester, or urethane reinforced by thin diameter fibers such as graphite, aramids, or boron. Because of their low cost, high strength, and simple manufacturing principles, PMCs are widely used. Low operating temperatures, high coefficients of thermal and moisture expansion, and low elastic properties in certain directions are some of the drawbacks of PMCs.

Glass, graphite, and Kevlar are the most commonly used fibers. The most common fiber used in polymer matrix composites is glass. Its benefits include high strength, low cost, chemical resistance, and good insulating properties. Low elastic modulus, poor adhesion to polymers, high specific gravity, sensitivity to abrasion (reduces tensile strength), and low fatigue strength are all disadvantages. E-glass (fiberglass) and S-glass are the two most common types of glass fibers. Because it was designed for electrical applications, the "E" in E-glass stands for electrical.

Furthermore, it is now used for a variety of other purposes, including decoration and structural applications. The "S" in S-glass denotes a higher silica content. S-glass fibers are stronger at high temperatures than E-glass fibers and have a higher fatigue strength. They are primarily used in aerospace applications. Other commercially available types include C-glass (Corrosion), which is used in chemical environments such as storage tanks; R-glass, which is used in structural applications such as construction; D-glass (Dielectric), which is used in applications requiring low dielectric constants such as radomes; and A-glass, which is used to improve surface appearance. There are also some combinational types, such as E-CR glass (Electrical and Corrosion resistance) and AR glass (Alkali Resistant).

Graphite fibers are increasingly used in high-modulus, high-strength applications such as aircraft components. Graphite fibers have high specific strength and modulus, as well as a low coefficient of thermal expansion and high fatigue strength. The drawbacks include high cost, low impact resistance, and high electrical conductivity.

An aramid fiber is a carbon, hydrogen, oxygen, and nitrogen aromatic organic compound. The benefits of aramid fiber include its low density, high tensile strength, low cost, and high impact resistance. Its drawbacks include low compressive properties and

deterioration in sunlight. Aramid fibers are classified into two types: Kevlar 29® and Kevlar 49®. Kevlar fibers have comparable specific strengths, but Kevlar 49 has a higher specific stiffness. Bulletproof vests, ropes, and cables are the most common applications for Kevlar 29. The aircraft industry uses Kevlar 49 in high-performance applications.

Polymers of various types are used in advanced polymer composites. These polymers include epoxy, phenolics, acrylic, urethane, and polyamide, and each has advantages and disadvantages in its application.

Furthermore, each resin system has advantages and disadvantages. The use of a specific resin system is determined by the application. These factors include mechanical strength, cost, smoke emission, temperature fluctuations, and so on. Figure 2.3 shows a comparison of five common resins based on smoke emission, strength, service temperature, and cost.

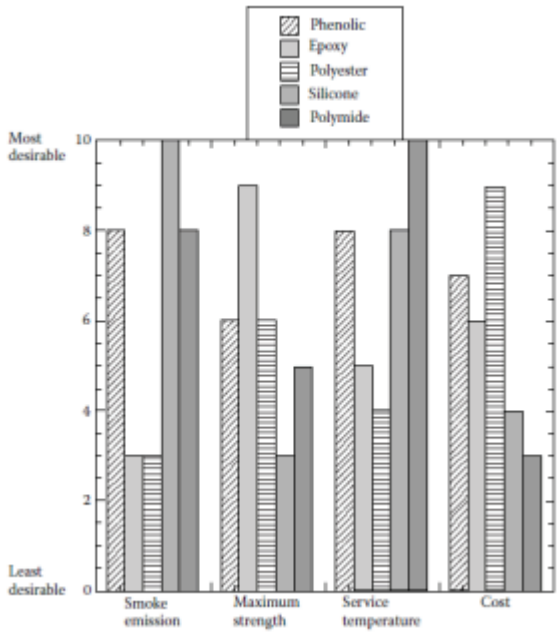

Figure 2.3. Performance comparison of several common matrices used in polymer matrix composites (Source: Kaw 2006)

The most popular resins are epoxy resins. They are organic liquids with low molecular weight that contain epoxide groups. In its molecule ring, epoxide has three members: one oxygen and two carbon atoms. The most common PMC matrix is epoxy, but it is more expensive than other polymer matrices. Epoxy makes up more than two-thirds of the polymer matrices used in aerospace applications. Epoxy resins are the most widely held PMC matrix and exist in more than 20 grades to meet specific property and processing requirements due to some advantages such as high strength, low viscosity, and

low flow rates, which allow good wetting of fibers and prevent misalignment of fibers during processing, low volatility during cure, and low shrink rates, which reduce the tendency of gaining large shear stresses of the bond between epoxy and its reinforcement.

Table 2.1. Differences between thermosets and thermoplastics
(Source: Kaw 2006)

Thermoplastics	Thermoset
Soften on heating and pressure and, thus easy to repair	Decompose on heating
High strains to failure	Low strains to failure
Indefinite shelf life	Definite shelf life
Can be reprocessed	Cannot be reprocessed
Not tacky and easy to handle	Tacky
Short cure cyclot	Long cure cycles
Higher fabrication temperature and viscosities have made it difficult to process	Lower fabrication temperature
Excellent solvent resistance	Fair solvent resistance

Thermosets and thermoplastics are two types of polymers. Because their molecular chains are rigidly joined with strong covalent bonds, thermoset polymers are insoluble and infusible after cure; thermoplastics are formable at high pressures and temperatures because their molecular bonds are weak and of the van der Waals type. Epoxies, polyesters, phenolics, and polyamide are examples of thermosets; polyethylene, polystyrene, polyether–ether–ketone (PEEK), and polyphenylene sulfide are examples of thermoplastics (PPS). Table 2.1 shows the distinctions between thermosets and thermoplastics (Kaw 2006).

2.2.1.3. Ceramic Matrix Composite Materials

Ceramic matrix composites (CMCs) are made up of a ceramic matrix like alumina calcium alumina silicate that is reinforced by fibers like carbon or silicon carbide. CMCs have the following advantages: high strength, hardness, high service temperature limits for ceramics, chemical inertness, and low density. Ceramics, on the other hand, have a low fracture toughness on their own. Under tensile or impact loading, ceramics fail catastrophically. The fracture strength of ceramics is increased by reinforcing ceramics with fibers such as silicon carbide or carbon, and the composite fails gradually as a result.

CMCs are more appealing for applications requiring high mechanical properties and extreme service temperatures due to the combination of fiber and ceramic matrix (Kaw 2006).

2.2.1.4. Carbon Carbon Matrix Composite Materials

Carbon-carbon composites(C/C) are made by combining carbon fibers with a carbon matrix such as graphite. This type of composite can be used in extremely high-temperature environments up to 3315°C, and it is 20 times stronger and 30% lighter than graphite fibers. Carbon, like ceramics, is inherently brittle and flaw-prone. Carbon matrix reinforcement allows the composite to fail gradually while also ensuring better properties such as high temperature resistance, low creep at high temperatures, low density, good tensile and compressive strengths, high fatigue resistance, high thermal conductivity, and high coefficient of friction. The major disadvantages of C/C composites are their high cost, low shear strength, and susceptibility to oxidation at high temperatures. (Kaw 2006).

C/C are a specialized but commercially important subclass of composite material formed by vapour infiltration of an array of carbon fibers. They are used not only in the long-standing application of aircraft brakes, but also in a variety of other aerospace industry components with stringent requirements (Kernel 2018).

2.3 Fiber Types

As reinforcements in structural applications, a wide range of fibers can be used. Fibers can be classified based on their length (short, long, or continuous fibers), strength and/or stiffness (low (LM), medium (MM), high (HM), and ultrahigh modulus (UHM), or chemical composition (organic and inorganic). Glass, carbon, boron, ceramic, mineral, and metallic fibers are the most common inorganic fibers used in composites. Polymeric fibers are the organic fibers used in composites. Choosing a fiber type necessitates a tradeoff between mechanical and environmental properties, as well as cost (Barbero 2010).

2.3.1. Carbon Fiber

Carbon fibers, also known as graphite fibers, are strong and lightweight fibers with excellent chemical resistance. They have a monopoly on the aerospace market. Carbon fibers' mechanical properties are determined by the atomic configuration of carbon chains and their connections, which is similar to graphite crystal structure. Carbon fiber strength is controlled by orienting the carbon atomic structures with their strongest atomic connections along the direction of the carbon fiber.

Carbon fiber qualities are determined by the raw material, the production process, and the specific manufacturing technique. Polyacrylonitrile (PAN) and pitch are the two main raw ingredients (precursors) used. Pitch fibers are less expensive than PAN fibers, but they are weaker. Pitch fibers have half the tensile strength and one-third the compressive strength of PAN fibers, owing to their inherent structure, which renders them more susceptible to surface flaws. Because they may be manufactured with a variety of stiffness and strength characteristics, PAN fibers dominate the high-performance market for aerospace applications (Barbero 2010).

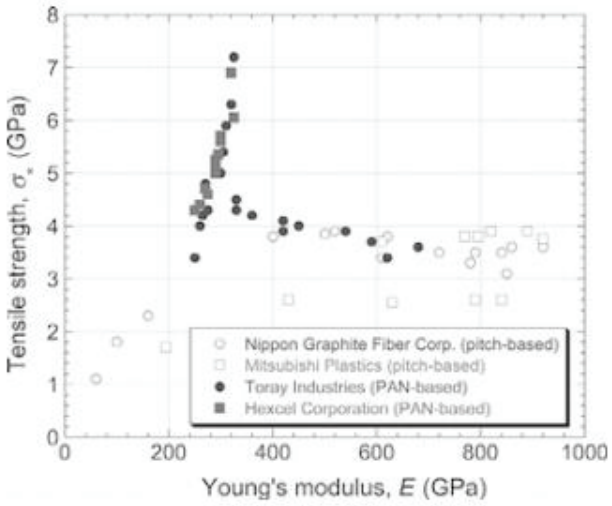

Figure 2.4. Performance comparison of several common matrices used in polymer matrix composites (Source: Tanaka 2018)

The carbon ring structure is then reduced from the oxidized PAN, which is subsequently transformed to turbostratic graphite by heating at higher temperatures (in

the absence of air – pyrolysing). A thin skin of circumferential basal planes surrounds a core of randomly arranged crystallites in most fibres (Cylne 2019).

2.3.2. Glass Fiber

Glass fibers are made from bulk glass, which is an amorphous substance made of sand, limestone, and other oxidic compounds. As a result, silica is the primary chemical constituent of glass fibers (46–75%). (SiO2). Controlling the chemical composition and manufacturing process yields a wide range of glass fibers for various applications, but they retain the typical glass properties of hardness, corrosion resistance, and inertness. They are also flexible, lightweight, and inexpensive. Because of these characteristics, glass fibers are the most widely used type of fiber in low-cost industrial applications.

The low number and size of defects on the surface of glass fibers contribute to their high strength. All glass fibers have a similar stiffness but differ in terms of strength and resistance to environmental degradation. E-glass fibers (E for electrical) are used in applications requiring high tensile strength and chemical resistance. Because of its mechanical performance, corrosion resistance, and low cost, e-glass is the preferred structural reinforcement material. S-glassTM and S-2-glassTM (S for strength) have the highest strength, but their application is limited because they are three to four times more expensive than E-glass. As a consequence, low-cost carbon fibers are now being considered as a viable alternative to S-glass and S-2-glass. C-glass (C for corrosion) is a corrosion-resistant material. D-glass (D for dielectric) is used in electrical applications such as the reinforcement of high voltage ceramic insulators' cores. For lightweight surfacing veils or mats, A-glass and AR-glass (alkaline resistant) are used. R-glass fiber is the European equivalent of S-glass fiber, which is used in high-performance applications in the United States. They are popular for filament winding and sheet molding compounds for high performance industrial applications due to their high modulus and strength, as well as very good temperature, humidity, and fatigue stability (Barbero 2010).

2.3.3. Organic Fibers

Among a wide range of organic fibers, polymeric fibers are particularly appealing for high-stiffness, high-strength structural applications, owing to their extremely low density, which results in extremely high specific strength and stiffness values (Barbero 2010).

Plant fibers are made up of cellulose, lignin, or similar compounds, whereas animal fibers are made up of protein. Pectin is the collective name for heteropolysaccharides, which give plants flexibility. Waxes are the final component of fibers and are made up of various types of alcohols (Ahmad 2014). Table 2.2 shows the chemical composition of a few natural fibers.

Table 2.2. List of important natural fibers (Source: Ahmad 2014)

Fiber source	Species	Origin
Abaca	*Musa textiles*	Leaf
Bamboo	(>1 250 species)	Grass
Banana	*Musa indica*	Leaf
Coir	*Cocos nucifera*	Fruit
Cotton	*Gossypium* sp.	Seed
Curauá	*Ananas erectifolius*	Leaf
Flax	*Linum usitatissimum*	Stem
Hemp	*Cannabis sativa*	Stem
Henequen	*Agave fourcroydes*	Leaf
Jute	*Corchorus capsularis*	Stem
Kenaf	*Hibiscus cannabinus*	Stem
Oil	*Elaeis guineensis*	Fruit
Pineapple	*Ananus comosus*	Leaf
Ramie	*Boehmeria nivea*	Stem
Sisal	*Agave sisilana*	Leaf
Wood	(>10 000 species)	Stem

2.3.4. Boron Fibers

Boron fibers have a high stiffness, a high strength, and a low density. They are most commonly used as reinforcement in aerospace and sports equipment. The statistical distribution of flaws during the manufacturing process determines the strength values.

Mechanical properties are maintained at high temperatures (typically, the tensile strength at 500°C is about 60% of the initial strength value at room temperature). They also have a high toughness, a high fatigue strength, and excellent compressive properties. They are fragile and have a low impact tenacity. Chemical vapor deposition on a tungsten wire produces boron fibers. Due to the obvious slow rate of production, boron fibers are among the most expensive of all the fibers currently manufactured, motivating the substitution of boron with carbon fibers whenever possible (Barbero 2010).

2.3.5. Ceramic Fibers

For high-temperature applications, ceramic fibers are used. Silicon Carbide (SiC) fibers are made in the same way as boron fibers, but on a carbon substrate. They are most commonly used as reinforcement for metal matrices, specifically titanium, but they have also been used in conjunction with temperature-resistant polymeric matrices. SiC fibers, like boron fibers, have high stiffness and strength, but they also have a higher temperature capability, as their initial tensile strength can be maintained at temperatures as high as 1300 degrees Celsius. The cost of these fibers is high due to their limited use and low production volumes.

Alumina fibers are made from the mineral alumina oxide Al2O3. They are not produced by chemical deposition, unlike other ceramic fibers, and thus have a high volume availability and a low cost (200 to 1100/kg depending on fiber type, tow size, and quantity). Ceramic fibers, which were originally used to reinforce diesel pistons, add strength and hardness to metal matrix composites at high temperatures, where metal properties typically degrade (Barbero 2010).

2.3.6. Basalt Fibers

Mineral fibers are what basalt fibers are. This new product is made from volcanic basalt rock that has been melted and extruded into fibers. Basalt fibers have better mechanical properties than glass fibers and are less expensive than carbon fibers. They have excellent thermal stability, high strength and stiffness, good chemical stability, corrosion resistance, and matrix adherence, and they are not affected by radiation. They could be used for thermal protection and structural applications (Lupescu 2004).

2.3.7. Metalic Fibers

Metallic fibers are made from a wide range of base metals and alloys. Flaws inherent in the bulk material are virtually eliminated and enhanced properties are achieved by processing the raw material into fibers of small dimensions of the order of a m. Fiber strength is proportional to fiber diameter, which is proportional to fiber manufacturing cost. The fiber material, such as lightweight aluminum fibers, strong steel fibers, or stiff tungsten fibers, can be chosen based on the application. Other benefits of these fibers include their high electrical and thermal conductivity. Metallic fibers are commonly utilized as filler nets in polymer matrices to give the final structural composite material electrical conductivity, electromagnetic interference protection, or lighting strike protection.

A wide range of new fibers are constantly introduced or improved, but market acceptance of new fiber products for structural applications is slow due to the large number of characterization tests required to ensure safe and effective application under a variety of conditions. While high strength-to-weight and stiffness-to-weight ratios are advantageous for aerospace applications, other properties of composites produced with these fibers are likely to be limiting factors in their application. Some of the limiting factors that must be investigated for any new material are environmental degradation, maximum operating temperature, transverse and shear strength (Barbero 2010).

CHAPTER 3

MECHANICS OF COMPOSITE MATERIALS

3.1 Introduction

Many engineers and material scientists are familiar with the behavior and design of isotropic materials, which include the metal family and pure polymers. The increased adoption of anisotropic materials, such as composites, has resulted in a materials revolution, requiring a new understanding of anisotropic material behavior.

Fiber-reinforced composite materials differ from conventional materials in application because the use of long fibers results in a material with a higher strength-to-density ratio and/or stiffness-to-density ratio than any other material system at moderate temperature, and the fiber orientations can be uniquely tailored to a given geometry, applied load, and environment (Mallick 2007).

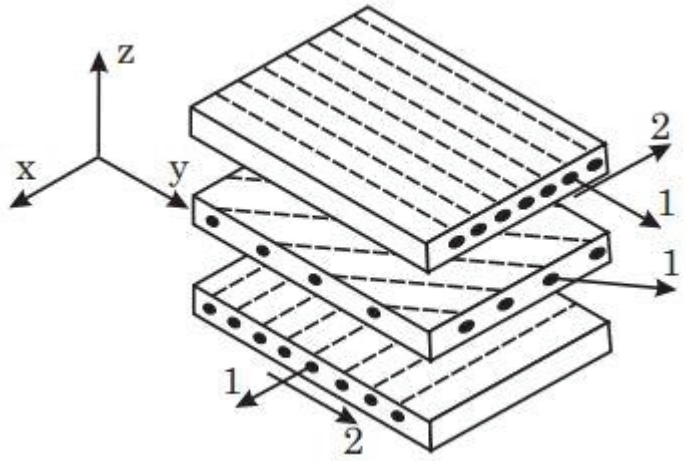

Figure 3.1. Assembly of lamination (Source: Barbero 2010)

The usage of fibers in short fiber composites, which are mostly employed in mass production and low-cost systems, makes the composites competitive and superior to plastic and metal alternatives. As a result, an engineer is not just a material selector, but also a material designer when using composite materials. Fiber-reinforced composites,

on the other hand, are microscopically inhomogeneous and orthotropic. As a result, fiber-reinforced composites have more sophisticated mechanics than conventional materials.

3.2. Classical Lamination Theory

Classical lamination theory is based on plate theory and is only applicable to thin laminates. It's used to study laminated structures' infinitesimal deformation. This theory assumes that the laminate is thin and wide, that perfect bounding exists between laminas, that a linear strain distribution exists through the thickness, that all laminas are macroscopically homogeneous and behave linearly elastically, and that the through-thickness and transverse shear strains are both zero.

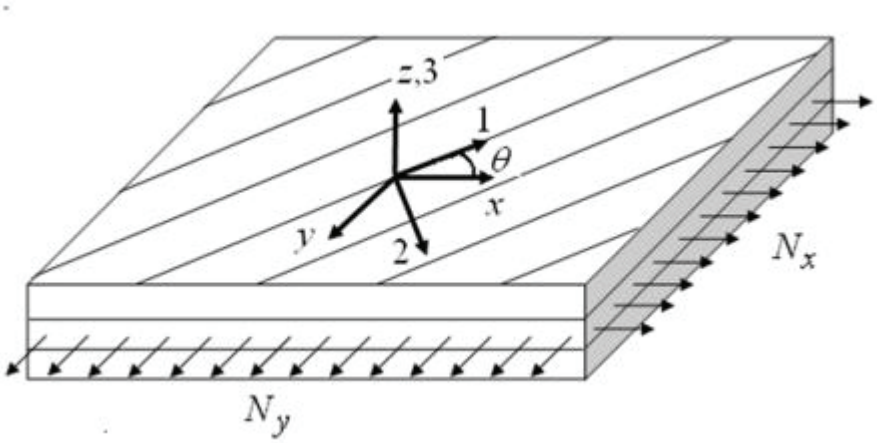

Figure 3.2. A thin fiber-reinforced laminated composite subjected to in plane loading (Source: Kaw 2006)

Figure 3.2 illustrates a thin laminated composite structure exposed to mechanical in-plane loading (N_x, N_y). The global coordinates of the layered material are defined by the Cartesian coordinate system x, y, and z. The fiber direction is aligned at an angle to the x axis in a layer-wise principal material coordinate system represented by 1, 2, 3. Figure 3.3 shows a representation of the lamination convention for an n-layered construction with a total thickness of h.

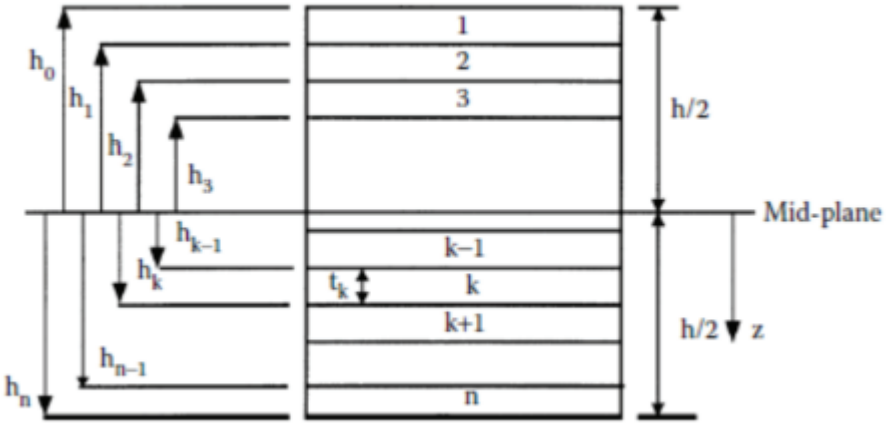

Figure 3.3. Schematic representation of a symmetric laminate
(Source: Kaw 2006)

Composite materials are typically applied in structural applications as thin laminates loaded in the plane of the laminate. As a result, composite laminates can be thought of as being under plane stress, with zero stress components in the out-of-plane direction (3-direction).

Based on the classical lamination theory, the stress-strain relationship for the k-th layer of a composite plate can be stated as follows:

$$\begin{bmatrix}\sigma_x\\ \sigma_y\\ \sigma_{xy}\end{bmatrix}_k = \begin{bmatrix}\bar{Q}_{11} & \bar{Q}_{12} & \bar{Q}_{16}\\ \bar{Q}_{12} & \bar{Q}_{22} & \bar{Q}_{26}\\ \bar{Q}_{16} & \bar{Q}_{26} & \bar{Q}_{66}\end{bmatrix}_k \left(\begin{bmatrix}\varepsilon_x^0\\ \varepsilon_y^0\\ \varepsilon_{xy}^0\end{bmatrix} + z \begin{bmatrix}\kappa_x\\ \kappa_y\\ \kappa_{xy}\end{bmatrix} \right)_k \tag{3.1}$$

where $[Q_{ij}]_k$ are the elements of the transformed reduced stiffness matrix, $[\varepsilon^0]$ is the mid-plane strains, respectively, $[\kappa]$ is curvatures.The transformed reduced stiffness matrix elements $[Q_{ij}]$ given in Eq. (3.1) can be follows

$$\bar{Q}_{11} = Q_{11}c^4 + Q_{22}s^4 + 2(Q_{12} + 2Q_{66})s^2c^2 \tag{3.2}$$

$$\bar{Q}_{12} = (Q_{11} + Q_{22} - 4Q_{66})s^2c^2 + Q_{12}(c^4 + s^4) \tag{3.3}$$

$$\bar{Q}_{22} = Q_{11}s^4 + Q_{22}c^4 + 2(Q_{12} + 2Q_{66})s^2c^2 \tag{3.4}$$

$$\bar{Q}_{16} = (Q_{11} - Q_{12} - 2Q_{66})sc^3 - (Q_{22} - Q_{12} - 2Q_{66})s^3c \quad (3.5)$$

$$\bar{Q}_{26} = (Q_{11} - Q_{12} - 2Q_{66})cs^3 - (Q_{22} - Q_{12} - 2Q_{66})sc^3 \quad (3.6)$$

$$\bar{Q}_{66} = (Q_{11} + Q_{22} - 2Q_{12} - 2Q_{66})s^2c^2 + Q_{66}(c^4 + s^4) \quad (3.7)$$

where stiffness matrix quantities [Q_{ij}] are

$$Q_{11} = \frac{E_1}{1-v_{21}v_{12}} \quad (3.8)$$

$$Q_{12} = \frac{v_{12}E_2}{1-v_{21}v_{12}} \quad (3.9)$$

$$Q_{22} = \frac{E_2}{1-v_{21}v_{12}} \quad (3.10)$$

$$Q_{66} = G_{12} \quad (3.11)$$

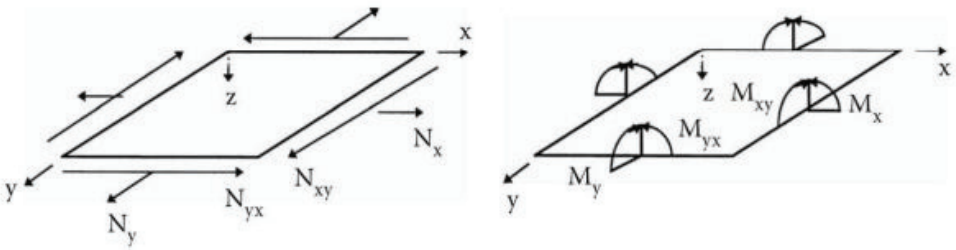

Figure 3.4 On a composite laminate, the resulting forces and moments (Source: Kaw 2006)

Applied normal force resultants N_x , N_y , shear force resultant N_{xy} (per unit width) and moment resultants M_x , M_y and M_{xy} on a laminate (Fig. 3.4) have the following relations:

$$\begin{bmatrix} N_x \\ N_y \\ N_{xy} \end{bmatrix} = \begin{bmatrix} A_{11} & A_{12} & A_{16} \\ A_{12} & A_{22} & A_{26} \\ A_{16} & A_{26} & A_{66} \end{bmatrix} \begin{bmatrix} \varepsilon_x^0 \\ \varepsilon_y^0 \\ \gamma_{xy}^0 \end{bmatrix} + \begin{bmatrix} B_{11} & B_{12} & B_{16} \\ B_{12} & B_{22} & B_{26} \\ B_{16} & B_{26} & B_{66} \end{bmatrix} \begin{bmatrix} \kappa_x \\ \kappa_y \\ \kappa_{xy} \end{bmatrix} \quad (3.12)$$

$$\begin{bmatrix} M_x \\ M_y \\ M_{xy} \end{bmatrix} = \begin{bmatrix} B_{11} & B_{12} & B_{16} \\ B_{12} & B_{22} & B_{26} \\ B_{16} & B_{26} & B_{66} \end{bmatrix} \begin{bmatrix} \varepsilon_x^0 \\ \varepsilon_y^0 \\ \gamma_{xy}^0 \end{bmatrix} + \begin{bmatrix} D_{11} & D_{12} & D_{16} \\ D_{12} & D_{22} & D_{26} \\ D_{16} & D_{26} & D_{66} \end{bmatrix} \begin{bmatrix} \kappa_x \\ \kappa_y \\ \kappa_{xy} \end{bmatrix} \tag{3.13}$$

The matrices [A], [B] and [D] specified in Equations 3.14, 3.15, 3.16 can be defined as:

$$A_{ij} = \sum_{k=1}^{n} \left[\left(\bar{Q}_{ij}\right)\right]_k (h_k - h_{k-1}), \quad i,j = 1,2,6 \tag{3.14}$$

$$B_{ij} = \frac{1}{2} \sum_{k=1}^{n} \left[\left(\bar{Q}_{ij}\right)\right]_k (h_k^2 - h_{k-1}^2), \quad i,j = 1,2,6 \tag{3.15}$$

$$D_{ij} = \frac{1}{3} \sum_{k=1}^{n} \left[\left(\bar{Q}_{ij}\right)\right]_k (h_k^3 - h_{k-1}^3), \quad i,j = 1,2,6 \tag{3.16}$$

The extensional, coupling, and bending stiffness matrices are the [A], [B], and [D] matrices, respectively. Combining Eqs. (3.12) and (3.13) yields six simultaneous linear equations and six unknowns as:

$$\begin{bmatrix} N_x \\ N_y \\ N_{xy} \\ M_x \\ M_y \\ M_{xy} \end{bmatrix} = \begin{bmatrix} A_{11} & A_{12} & A_{16} & B_{11} & B_{12} & B_{16} \\ A_{12} & A_{22} & A_{26} & B_{12} & B_{22} & B_{26} \\ A_{16} & A_{26} & A_{66} & B_{16} & B_{26} & B_{66} \\ B_{11} & B_{12} & B_{16} & D_{11} & D_{12} & D_{16} \\ B_{12} & B_{22} & B_{26} & D_{12} & D_{22} & D_{26} \\ B_{16} & B_{26} & B_{66} & D_{16} & D_{26} & D_{66} \end{bmatrix} \begin{bmatrix} \varepsilon_x^0 \\ \varepsilon_y^0 \\ \gamma_{xy}^0 \\ \kappa_x \\ \kappa_y \\ \kappa_{xy} \end{bmatrix} \tag{3.17}$$

The resultant in-plane forces are related to in-plane strains by the extensional stiffness matrix [A], and the resultant bending moments are related to plate curvatures by the bending stiffness matrix [D]. The mid-plane strains and mid-plane curvatures are coupled to the force and moment terms by the coupling stiffness matrix [B] (Kaw 2006).

Stresses and strains based on traditional lamination theory can now be described using a local coordinate system (1, 2). In an angled lamina, the relationship between local and global stresses can be stated as follows:

$$\begin{bmatrix}\sigma_1\\ \sigma_2\\ \sigma_{12}\end{bmatrix} = [T]\begin{bmatrix}\sigma_x\\ \sigma_y\\ \sigma_{xy}\end{bmatrix} \tag{3.18}$$

The local and global strains are also linked in the following way,

$$\begin{bmatrix}\varepsilon_1\\ \varepsilon_2\\ \varepsilon_{12}\end{bmatrix} = [R][T][R]^{-1}\begin{bmatrix}\varepsilon_x\\ \varepsilon_y\\ \varepsilon_{xy}\end{bmatrix} \tag{3.19}$$

where

$$[R] = \begin{bmatrix}1 & 0 & 0\\ 0 & 1 & 0\\ 0 & 0 & 2\end{bmatrix} \tag{3.20}$$

[T] is a transform matrix,

$$[T] = \begin{bmatrix}c^2 & s^2 & 2sc\\ s^2 & c^2 & -2sc\\ -sc & sc & c^2 - s^2\end{bmatrix} \quad c = cos\theta, s = sin\theta \tag{3.21}$$

3.3 Buckling Theory of Laminated Composite Plates

Engineers, scientists, and manufacturers have become more interested in fiber-reinforced composites as a result of its remarkable stiffness and weight qualities. During service, the composite laminate plates are often subjected to compression loads, which might induce buckling if they are overloaded. Their buckling characteristics are also important factors in the building of safe and stable systems (Baba 2007).

A structural component made of stiffened sheet panels will not fail when the panel skin buckles because the stiffening units can usually withstand more loading before failing. However, in many design situations, the initial buckling of panel skin must meet certain design specifications or criteria. For instance, the top surface skin of a low wing passenger airplane should not buckle under accelerations caused by air gusts encountered during normal everyday flying, preventing passengers from observing wing skin buckling in normal flying conditions. Another example would be that no buckling of fuselage skin

panels should occur while a commercial airplane is on the ground with a full load aboard to prevent the public from witnessing buckling of fuselage skin. In some cases, aerodynamic or rigidity requirements may prevent panel skin from buckling. To ensure that buckling does not occur under certain load requirements, it is best to be conservative when selecting or calculating the sheet panel boundary restraints (Chun 2011).

Assuming that the composite plate in Figure 3.2 is loaded by N_x, N_y, and N_{xy} in-plane compressive loads, where is a scalar amplitude parameter and the plate is simply supported on four sides, the governing differential equation for the plate's buckling behavior, using classical plate theory, is

$$D_{11}\frac{\partial^4 w}{\partial x^4} + 2(D_{12} + 2D_{66})\frac{\partial^4 w}{\partial x^2 \partial y^2} + D_{22}\frac{\partial^4 w}{\partial y^4} = \lambda\left(N_x\frac{\partial^2 w}{\partial x^2} + N_y\frac{\partial^2 w}{\partial y^2} + N_{xy}\frac{\partial^2 w}{\partial x \partial y}\right) \quad (3.22)$$

where D_{11}, D_{12}, D_{22}, D_{66} are bending stiffness factors, and w is the vertical displacement;

$$w(x,y) = \sum_m \sum_n A_{mn} sin\frac{m\pi x}{a} sin\frac{n\pi y}{b} \quad (3.23)$$

The buckling load factor expression can be determined by substituting Equation 3.23 for Equation 3.22 as shown below.

$$\lambda_b = \frac{\pi^2\left[D_{11}\left(\frac{m}{a}\right)^4 + 2(D_{12}+2D_{66})\left(\frac{m}{a}\right)^2\left(\frac{n}{b}\right)^2 + D_{22}\left(\frac{n}{b}\right)^4\right]}{N_x\left(\frac{m}{a}\right)^2 + N_y\left(\frac{n}{b}\right)^2 + N_{xy}\left(\frac{m}{a}\right)\left(\frac{n}{b}\right)} \quad (3.24)$$

D_{16} and D_{26} are not included in Equations 3.22 and 3.23 because they are zero for a specifically orthotropic laminate and small in comparison to the other D_{ij}'s for a symmetric laminate with a number of laminas of ply angles in sequence (Karakaya and Soykasap 2009).

When the magnitude parameter hits a critical value of λ_b, the laminate buckles into m and n half-waves in the x and y axes, respectively (Spallino and Thierauf 2000). The critical buckling load factor λ_{cb} is the smallest value of λ_b under proper m and n values, and it restricts the maximum load that the laminate can bear without buckling. The crucial

values of m and n are modest unless the plate has a very high aspect ratio or excessive D_{ij}'s ratios (Gurdal, et al 1999).

$$\lambda_{cb} = \min \lambda_{cb}(m,n) \tag{3.25}$$

The critical buckling load factor λ_{cb} varies with the plate aspect ratio, loading ratio, and material, and should be greater than one to avoid any unexpected failure. According to ANSI 360-16, the minimum critical buckling in composite beams should be greater than 3.

3.4. Eigenvalue Buckling Analysis in ANSYS

The theoretical buckling strength of an ideal elastic structure can be predicted using an Eigenvalue Buckling analysis. This method is similar to the textbook approach to elastic buckling analysis: an eigenvalue buckling analysis of a column, for example, is equivalent to the classical Euler solution. Most real-world structures, however, are unable to achieve their theoretical elastic buckling strength due to defects and nonlinearities. As a result, Eigenvalue Buckling analysis frequently produces non-conservative conclusions.

A nonlinear buckling analysis is a more accurate method of anticipating instability. This entails performing a static structural analysis with large deflection effects enabled. This analysis uses a progressively increasing load to find the load level at which your structure becomes unstable. Your model can include elements like initial defects, plastic behavior, gaps, and largedeflection response using the nonlinear approach. In addition, the post-buckling performance of the structure can also be monitored using yaw-controlled loading, which is important in situations where the structure has shifted to a stable state, such as the interlaced buckling of a shallow dome, as can be seen below in Figure 3.5.

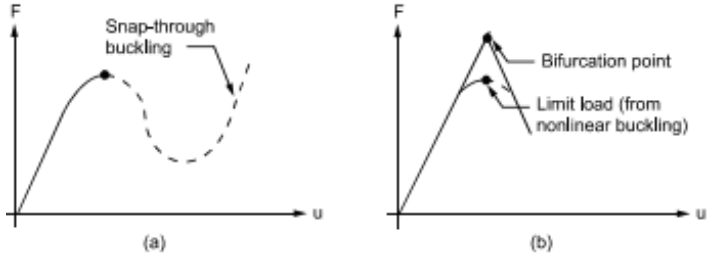

Figure 3.5 (a) Nonlinear load-deflection curve, (b) Eigenvalue buckling curve (Source: Kolakowski 2005)

The linear perturbation approach is used in eigen buckling analysis, which is based on a basic eigenvalue problem. The linear perturbation analysis approach is used to solve a linear issue based on its preloaded linear or nonlinear state. The previous linear or nonlinear analysis is referred to as the basis analysis. The impacts from the base analysis are "frozen" in the perturbation analysis and can be reused in current or future study scenarios. For the eigen buckling analysis, looking at the governing equation of the eigenvalue problem.

$$([K_t] + \lambda_i[S])\{\Psi_i\} = 0 \tag{3.26}$$

where λ_i are the eigenvalues and Ψ are the eigenvectors. Examine the K_t and S matrices. Instead of the initial total stiffness matrix, the K_t matrix could be the total tangent matrix from the load point of interest. The linear perturbed stress stiffening matrix is denoted by S. The stiffening of a structure as a result of its stress condition is known as stress stiffening. The terms eigenvalue λ and eigenvector Ψ are used in this equation. The load factors or buckling load magnitudes are the solution λ in this case and Ψ stands for the buckling modes. There may be more than one method for the structure to buckle under the given weights, as shown by the subscript "i." Engineers are frequently interested in a structure's initial few buckling modes.

The buckling load is calculated by multiplying the applied loads by the buckling load factor when the basis analysis is a linear analysis. The perturbed load $F_{perturbed}$ in linearbased eigenvalue buckling analysis equals the applied load in the base analysis. The buckling load is estimated differently when the base analysis is nonlinear, such as when material, geometric, or contact nonlinearities exist.

Base analysis is linear,

$$\{F_{buckling}\} = \lambda_i\{F_{perturbed}\} \tag{3.27}$$

Base analysis is nonlinear,

$$\{F_{buckling}\} = \{Fbase\} + \lambda_i\{F_{perturbed}\} \tag{3.28}$$

In an eigen buckling analysis with a nonlinear ground state, a different distortion load can be defined in the buckling analysis compared to the loads applied in the nonlinear base analysis. As a result, the λ load multiplier scales only the loads used in the buckling analysis. The sum of the load imposed in the nonlinear base analysis and the scaled perturbation load is the total buckling load.

The various methods for estimating the buckling load in Eigen Buckling analyses based on either a linear or nonlinear analysis, as doing so improperly can result in mistakes in determining the actual buckling load. In general, Eigen Buckling analysis is a very effective method of predicting a structure's buckling stresses and associated buckling modes. It's the first stage in any investigation into instabilities or buckling. Despite the fact that it's a linear analysis that estimates the unconservative theoretical buckling strength, it tells us whether a structure can buckle in more than one way. This approach can also be used to discover and evaluate potential global and local buckling modes. A thorough nonlinear buckling analysis can't provide this information because it only provides one buckling solution (ANSYS 2020).

In this study, firstly, linear buckling analysis was performed to determine the critical buckling load and corresponding buckling mode shapes. Such calculations enabled the beam buckling load value to be found. Next, nonlinear analysis of structure stability was performed to find the solution to fracture in the post-buckling range. Thus, the first local mode shape obtained in the nonlinear buckling analysis was mapped onto the nodal mesh of the finite element model to generate the imperfect walls of the beam.

CHAPTER 4

FAILURE THEORIES

Weight reduction in composite beams necessitates strength limitations, since a reduction in the number of load-bearing plies eventually leads to failure. Composite structures must be able to withstand the applied loads without failing. As a result, many academics have been interested in the topic of failure criteria for fiber-reinforced plastic composites in recent decades. Various methodologies have been published in the literature that clearly demonstrate failure criteria for fiber-reinforced composites, and this subject remains an essential study topic in composite constructions.

Limit or non-interactive theories (e.g., Maximum stress or maximum strain), interactive theories (e.g., Tsai-Hill, Tsai-Wu, or Hoffman), and partially interactive or failure mode-based theories (e.g., Hashin, Puck failure criterion) are the three types of failure criteria for composite plates (Lopez, et al. 2009).

4.1. Traditional Failure Theories

The most often utilized failure criteria for polymer-matrix composites must be specified. The maximal stress and the Tsai-Wu criterion are these. These theories of failure presume that failure only happens in the fiber direction.

4.1.1. Maximum Stress Theory

The stresses in each lamina in the major material coordinates are used to analyze the failure of laminated composites. This theory is comparable to those used to isotropic materials, such as Rankine's maximum normal stress theory and Tresca's maximum shearing stress theory. The normal and shear stresses in the local axes are resolved from the stresses occurring on a lamina. Failure occurs when the maximum stress in the major material coordinates exceeds the respective strength, according to the maximum stress theory. This is written as,

$$\sigma_1 \geq X_T \quad \text{or} \quad \sigma_2 \geq Y_T \qquad \text{(tensile stresses)} \tag{4.1}$$

$$\sigma_1 \leq -X_c \quad \text{or} \quad \sigma_2 \geq -Y_c \qquad \text{(compressive stresses)} \tag{4.2}$$

$$\tau_{12} \geq S_{12} \qquad \text{(shearing stresses)} \tag{4.3}$$

where the normal stresses in σ_1 and σ_2 are directions 1 and 2, respectively; X_T and X_C are the tensile and compressive strengths parallel to the fiber direction, respectively; Y_T and Y_C are the tensile and compressive strengths normal to the fiber direction, respectively; and S_{12} is the shear strength in the elastic symmetry plane 1-2. It's worth noting that X_T, X_C, Y_T, Y_C, and S_{12} are all positive numbers (Kaw, 2006)

4.1.2. Tsai-Wu Failure Criterion

One of the most extensively used failure criteria for anisotropic materials like unidirectional composites is the Tsai-Wu failure criterion. Over the years, researchers and designers have applied it to a variety of composite engineering constructions. It's also been included into commercial finite element software products like Abaqus and ANSYS with great success.

With orthotropic materials, the Tsai–Wu criterion is proposed. It is based on Beltrami's total strain energy failure theory and is derived from von Mises' yield criterion. Tsai-Wu extended the failure theory to a plane-stressed lamina. If a lamina fails, it is deemed a failure (Kaw 2006)

$$FI = F_1\sigma_1 + F_2\sigma_2 + F_3\sigma_3 + F_{11}\sigma_1^2 + F_{22}\sigma_2^2 + F_{33}\sigma_3^2 + F_{44}\sigma_4^2 + F_{55}\sigma_5^2 + F_{66}\sigma_6^2 + 2F_{12}\sigma_1\sigma_2 + 22F_{13}\sigma_1\sigma_3 + 2F_{23}\sigma_2\sigma_3 < 1 \tag{4.4}$$

where

$$F_1 = \frac{1}{X_t} + \frac{1}{X_c};\ F_2 = \frac{1}{Y_t} + \frac{1}{Y_c};$$

$$F_3 = \frac{1}{Z_t} + \frac{1}{Z_c}; F_{11} = -\frac{1}{X_t X_c};$$

$$F_{22} = -\frac{1}{Y_t Y_c}; F_{33} = -\frac{1}{Z_t Z_c};$$

$$F_{44} = \frac{1}{S_{23}^2};\ F_{55} = \frac{1}{S_{13}^2}; \tag{4.5}$$

$$F_{66} = \frac{1}{S_{12}^2}; F_{12} = -\frac{\sqrt{F_{11}F_{12}}}{2};$$

$$F_{23} = -\frac{\sqrt{F_{22}F_{33}}}{2}; F_{13} = -\frac{\sqrt{F_{11}F_{33}}}{2}$$

4.1.3. Tsai - Hill Failure Criterion

This theory is based on Von-Mises' distortional energy yield requirement for isotropic materials as applied to anisotropic materials' distortion energy failure theory. Distortion energy is a component of a body's overall strain energy. The strain energy in a body is divided into two parts: the dilatation energy, which is caused by a change in volume, and the distortion energy, which is caused by a change in shape (Kaw, 2006).

$$\left[\frac{\sigma_1}{(\sigma_1^T)_{ult}}\right]^2 - \left[\frac{\sigma_1\sigma_2}{(\sigma_1^T)_{ult}^2}\right] + \left[\frac{\sigma_2}{(\sigma_2^T)_{ult}}\right]^2 + \left[\frac{\tau_{12}}{(\tau_{12})_{ult}}\right]^2 < 1 \tag{4.6}$$

4.1.4. Puck Failure Criterion

The composite plate Puck Failure Theory is based on Mohr's idea that fracture is induced solely by stresses operating on the fracture plane. There are two basic failure scenarios in Puck faillure theory; fiber theory and inter - fiber failure.

Fiber failure is predicated on the premise that failure occurs at the same threshold level for multiaxial loads σ_{f1} and σ_{f2} as it does for uniaxial strains. Following considerable progress, Puck and Schürmann discovered that failure happens when one of the following conditions is met:

For tensile stress,

$$\frac{1}{\varepsilon_{1T}}\left(\varepsilon_1 + \frac{\nu_{f12}}{E_{f1}} m_{\sigma f}\sigma_2\right) = 1 \qquad for\ S \geq 0 \tag{4.7}$$

For compressive stresses,

$$\frac{1}{\varepsilon_{1C}}\left|\left(\varepsilon_1 + \frac{\nu_{f12}}{E_{f1}} m_{\sigma f}\sigma_2\right)\right| + (10\gamma_{21})^2 = 1 \qquad for\ S < 0 \tag{4.8}$$

in which,

$$S = \left(\varepsilon_1 + \frac{\nu_{f12}}{E_{f1}} m_{\sigma f}\sigma_2\right) \tag{4.9}$$

where ε_{1T} and ε_{1C} are the tensile and compressive failure strains in direction 1; ε_1 is the normal strain in direction 1; and ν_{f12} is the fibers' Poisson's ratio (the ratio of the strain in direction 2 to the strain in direction 1, both of which are caused by a stress in direction 1 only); m_{cf} accounts for a stress-magnification effect caused by the different moduli of the fibers and matrix in direction 2, resulting in an uneven distribution of the stress σ_2 from a micromechanical standpoint; E_{f1} is the Young's modulus of the fiber in direction 1; and γ_{21} is the shear strain in planes 1-2, with $(10\gamma_{21})^2$ being an empirical shear correction. It is worth noting that S≥0 corresponds to tension, whereas S < 0 corresponds to compression (Puck 2002).

Interfiber failure equations are determined using the axes corresponding to the failure plane, rather than the principal material coordinates (Figure 4.1). Figure 4.1 depicts these axes, with θ_{fp} denoting the angle at which failure occurs.

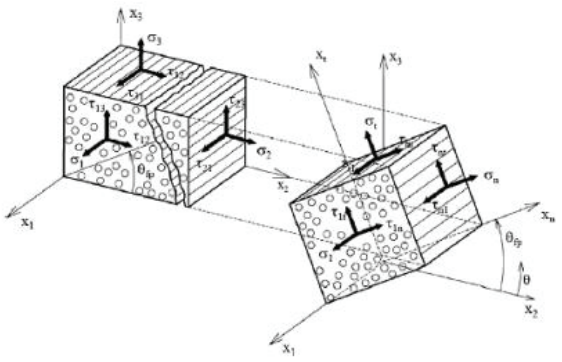

Figure 4.1. Stresses in three dimensions on a UD composite part
(Source: Lopez, et al. 2009).

The fiber direction (x_1), laminate mid-surface (x_2), and thickness direction (x_3) coordinate systems are fixed (x_3). The coordinate system (x_1, x_n, x_t) is rotated by an angle θ_{fp} from the x_2 to the x_n, which is normal to the fracture plane. According to Mohr's strength theory, only the three stresses σ_n, σ_{nt}, and σ_{n1} effect inter-fiber fracture (Source: Puck and Schürmann 2002).

The PFC not only offers a failure factor, but also the inclination of the plane where failure may occur, allowing for a considerably more accurate assessment of the effects of Inter Fiber Failure(IFF) in the laminate. The failure modes of IFF are A, B, and C. Figure 4.2 depicts this.

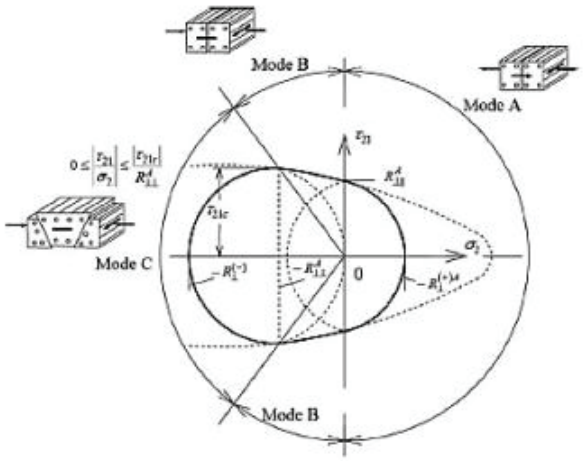

Figure 4.2. (σ_2, τ_{21}) fracture curve for σ_1, representing the three different fracture modes (A, B and C) for the PFC (Source: Lopez, et al. 2009)

When the lamina is subjected to tensile transverse stress, mode A occurs; nevertheless, compressive transverse stress occurs in modes B and C. The premise behind mode classification is that tensile stress $\sigma_n > 0$ causes fracture, but compressive stress $\sigma_n < 0$ prevents shear fracture. For $\sigma_n < 0$, the shear stresses τ_{nt} and τ_{n1} or just one of them must contend with an extra fracture resistance, which raises $|\sigma_n|$ in the same way that internal friction does.

It is vital to employ criteria that closely resemble the real behavior of the laminated composites under investigation. Many research on the best composite design use failure criteria based on the von Mises or Hill yield criterion, which are more suited to ductile

materials. Because the failure behavior of composite parts is comparable to that of brittle materials, such as Mohr's criterion, it is more acceptable to utilize criteria designed for materials with brittle fractures.

4.1.5 Hoffman Failure Criterion

Hoffman created a failure criterion by adding linear terms to Hill's criterion. The Hoffman criterion, like the Tsai-Hill failure criterion, is a stress-based, quadratic, failure mode independent criterion that takes stress interaction into consideration. Hoffman's theory may be applied to an orthotropic lamina with uneven tensile and compressive strengths, with the equation being (Hoffman 1960):

$$\frac{\sigma_{11}}{X_t} - \frac{\sigma_{11}}{X_c} + \frac{\sigma_{22}}{Y_t} - \frac{\sigma_{22}}{Y_c} + \frac{\sigma_{11}^2 - \sigma_{11}\sigma_{22}}{X_t X_c} + \frac{\sigma_{22}^2}{Y_t Y_c} + \frac{\tau_{12}^2}{S_{12}^2} \geq 1 \tag{4.10}$$

4.1.6 Hashin Failure Criterion

Hashin failure criteria discriminate between the various failure modes of the unidirectional lamina: tensile and compressive fiber failures, as well as tensile and compressive matrix failures, and are listed separately for each of these failure modes as follows:

Tensile Fiber Mode: $\sigma_1 > 0$

$$\left(\frac{\sigma_1}{X^t}\right)^2 + \left(\frac{\tau_{12}}{S}\right)^2 = 1 \tag{4.11}$$

Compressive Fiber Mode: $\sigma_1 < 0$

$$\sigma_1 = X^c \tag{4.12}$$

Tensile Matrix Mode: $\sigma_2 > 0$

$$\left(\frac{\sigma_2}{Y^t}\right)^2 + \left(\frac{\tau_{12}}{S}\right)^2 = 1 \tag{4.13}$$

Compressive MatrixMode: $\sigma_2 < 0$

$$\left(\frac{\sigma_2}{2S^T}\right)^2 + \left[\left(\frac{Y^T}{2S^T}\right)^2 - 1\right]\frac{\sigma_2}{Y^c} + \left(\frac{\tau_{12}}{S}\right)^2 \tag{4.14}$$

where S^T denotes transverse or out-of-plane shear strength, S denotes longitudinal or in-plane shear strength, and the others have already been defined. Hashin failure criteria are quadratic polynomials of stresses, just like Tsai-Hill failure criteria. They are, however, constructed from general polynomials of the first four transversely isotropic stress invariants, with the highest order term for each of these four invariants chosen in a way that results in a quadratic highest order of stress. As a result, Hashin failure criteria only define a piecewise smooth failure envelope, with each smooth branch modeling a different failure mode. The Hashin criteria increase the accuracy of intralamina failure prediction. However, as Hashin points out, the quadratic matrix mode failure criteria assume that the fracture plane is the maximum transverse shear plane, which is not necessarily the case. To get over this constraint, Hashin proposes a more generic technique based on the Mohr-Coulomb failure theory for matrix failure (Duong et. Al., 2016).

In this study the Tsai-Wu failure criterion was utilized to identify the first ply failure in the hybrid composite lamina.

CHAPTER 5

OPTIMIZATION

5.1. Introduction

Optimization is widely used in a variety of industrial fields, including aerospace, automotive, biomedicine, and so on. Engineers are always looking for appropriate solutions that provide the highest quality while meeting design requirements with limited resources. These solutions, however, are not easily achievable. In this sense, optimization methods have emerged as popular and powerful methods for solving complex engineering optimization problems in recent years.

The act of obtaining the best result under given circumstances in order to identify the best candidate from a collection of alternatives is known as optimization. The primary goal of optimization is to either minimize the effort required or maximize the desired benefit. Because the effort or benefit desired in any practical situation can be expressed as a function of certain decision variables, optimization can be defined as the process of determining the conditions that give the maximum or minimum value of a function (Rao 2019).

In recent decades, modern optimization methods have emerged as powerful and popular methods for solving complex engineering optimization problems. Genetic algorithms, simulated annealing, particle swarm optimization, ant colony optimization, neural network-based optimization, and fuzzy optimization are examples of optimization methods.

The genetic algorithm, one of the most widely used optimization methods, is a computerized search and optimization algorithm based on the mechanics of natural genetics and natural selection. John Holland proposed the first genetic algorithms in 1975 (Deveci 2016).

The act of obtaining the best result under given conditions is known as optimization. The ultimate goal of any engineering system design is to either minimize the effort required or maximize the desired benefit. Because the amount of effort required or the

benefit anticipated in any practical situation can be expressed as a function of certain decision variables, optimization can be defined as the process of determining the conditions that give the maximum or minimum value of a function. Figure 5.1 shows that if a point x^* corresponds to the minimum value of the function $f(x)$, that same point also corresponds to the maximum value of the function's negative, $-f(x)$. As a result, optimization can be taken to mean minimization without loss of generality, because the maximum of a function can be found by searching for the minimum of the negative of the same function (Rao 2019).

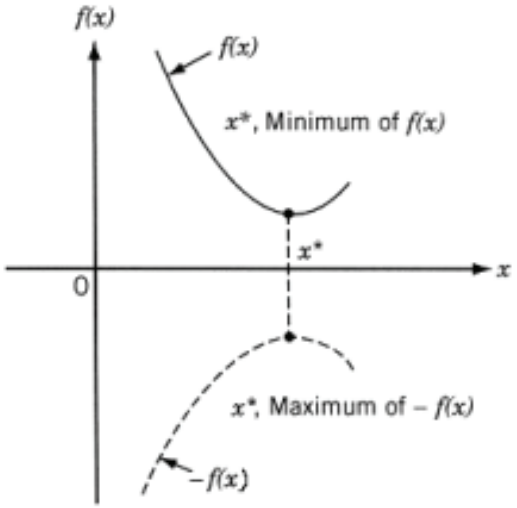

Figure 5.1 On a composite laminate, the resulting forces and moments
(Source: Rao 2019)

The optimization methods are useful in determining the minimum of a function of several variables given a set of constraints. To analyze problems defined by a set of random variables with known probability distributions, stochastic search techniques can be used. Statistical methods enable the analysis of experimental data and the development of empirical models in order to achieve the most accurate representation of the physical situation. The genetic algorithms that we are interested in fall under the category of modern optimization techniques, and they are the most widely used one (Rao 2019).

5.2.Definition of Optimization Problem

The following is a definition of an optimization or mathematical programming problem:

$$\text{Find } X = \begin{Bmatrix} x_1 \\ x_2 \\ . \\ . \\ x_n \end{Bmatrix} \text{ which minimizes f(x)} \quad (5.1)$$

depending on the conditions

$$g_j(X) \leq 0 \qquad i = 1,2,\ldots,m \quad (5.2)$$

$$l_k(X) = 0 \qquad k = 1,2\ldots.,p \quad (5.3)$$

here X is an n-dimensional vector known as the design vector, $f(X)$ is the objective function, and $g_i(X)$ and $l_i(X)$ respectively, are inequality and equality constraints. There is no requirement that the number of variables n and the number of constraints m and/or p be connected in any way. Equation 4.1's optimization problem is known as a constrained optimization problem. Some optimization problems, referred to as unconstrained optimization problems, have no restrictions (Rao 2019).

5.3. Genetic Algorithm (GA)

Nature-inspired algorithms, such as the Genetic Algorithm (GA), are gaining traction in solving difficult engineering issues. To solve difficult non-linear problems, GA develops a set of mathematical equations. GA is a form of Genetic Algorithm that was first introduced by Koza (1992) and employs machine-learning techniques to symbolically maximize a set of mathematical answers by utilizing Darwinian natural selection. The GA technique uses three primary processes to simulate biological evolution of survival of the fittest: selection or reproduction, crossover, and mutation employing a population of viable solutions. A simple kind of link between ndependent and dependent variables is assumed in a regression method. The model's parameters are then chosen so that it best fits the data. This is one of the drawbacks of traditional regression methods, which use a fixed polynomial function in the analysis.

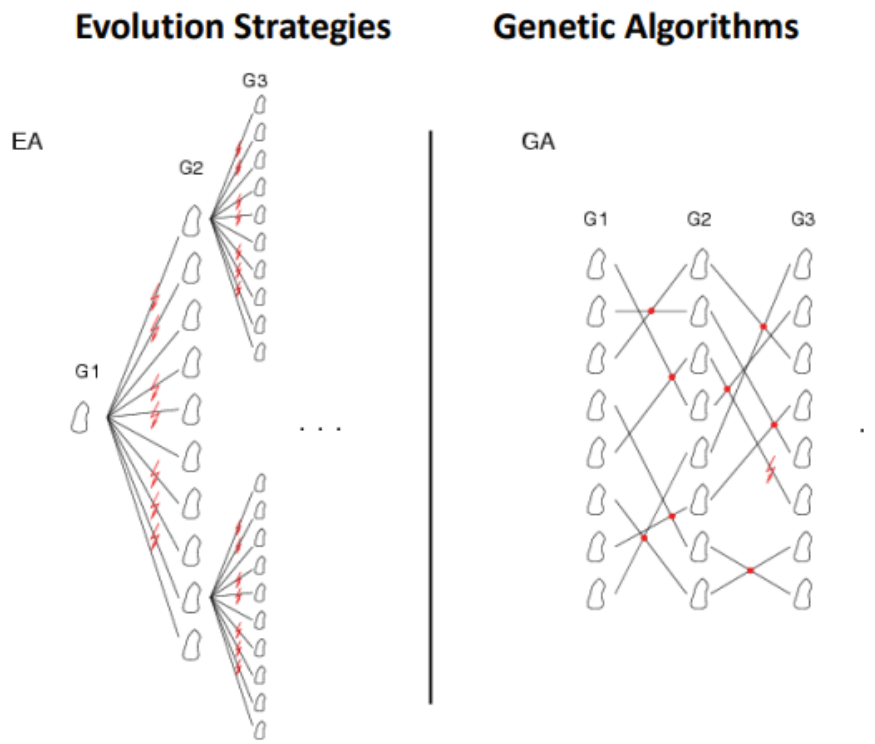

Figure 5.2 Tree for Genetic Algorithm and Evolutionary Strategies.
(Source: ANSYS 2020)

GA is a hierarchical mathematical model whose goal is to discover a solution within the population by searching for the best fit. By searching, the problem is brought closer to a global optimum solution. The starting population is created using a random search that is defined by the problem to be solved (Shahnewaz 2020).

In Figure 5.2, the difference between genetic algorithm and evolutionary strategy is given visually. Evolutionary algorithms (EA) are stochastic search methods that imitate processes like adaptation, selection, and variation found in actual biological evolution. The manner variation is introduced to the population is the major distinction between the two main versions, genetic algorithms (GA) and evolution strategies (ES). Within GA, recombination of genes utilizing crossover operators is the most common variation, whereas mutation introduces diversity to the population in evolution techniques. optiSLang employs a flexible implementation of the GA and ES, allowing scaling between pure GA and pure ES, which execute global and local searches, respectively. A start population is created randomly using Latin Hypercube Sampling for a worldwide search, or multiple designs might be chosen from earlier analyses.

In an ideal scenario, the best designs are derived from a previous sensitivity study. A single starting design is required for a local search, and design improvement is achieved via local crossover and mutation processes similar to those used in ES. For discrete and continuous design variables, single and multi-objective optimization tasks, and challenges with a high ratio of rejected designs, evolutionary methods can be applied. If the number of design variables and constraint conditions is large, EA is much more efficient than gradient-based and response surface-based techniques (ANSYS 2020).

5.4. Meta-model of Optimal Prognosis (MOP)

The Metamodel of Optimal Prognosis (MOP) was created by Dynardo as an automated method for determining the best filter meta-model configurations (Most 2008). This allows a surrogate model of the actual physical problem to be used to test various design configurations without having to run any further analysis. To create an automatic approach, you must first specify a metric for describing estimate quality. This allows a surrogate model of the actual physical problem to be used to test various design configurations without having to run any further analysis. To create an automatic approach, you must first specify a metric for describing approximation quality. The MOP employs the generalized coefficient of determination (CoD), which yields pure polynomial regression as a specific instance. The CoD measures the proportional amount of variance explained by the approximation to assess the approximation quality of a polynomial regression:

$$R^2 = \frac{SS_R}{SS_T} = 1 - \frac{SS_E}{SS_T};\ 0 \le R^2 \le 1 \tag{5.4}$$

when SS_T represents total variation, SS_R represents regression variation, and SS_E represents unexplained variance in the following way:

$$SS_T = \sum_{i=1}^{N} (y_i - \mu_Y)^2,\ SS_R = \sum_{i=1}^{N} (\hat{y}_i - \mu_{\hat{Y}})^2,\ SS_E = \sum_{i=1}^{N} (y_i - \hat{y}_i)^2 \tag{5.5}$$

Nevertheless, in order to penalize over-fitting, the modified CoD was established, as shown in Equation 5.6,

$$R^2_{adj} = 1 - \frac{N-1}{N-p}(1 - R^2) \tag{5.6}$$

The number of sample points is *N*, and the number of regression coefficients is *p*. Using an additional test data set, the quality of an approximation was assessed in terms of prognostic quality. The coefficient of prognosis measures the agreement between the real test data and the meta-model estimates. CoP by Most (2008) defined as in Equatation 5.7.

$$CoP = \left(\frac{E|Y_{test} * \hat{Y}_{test}|}{\sigma_{Y_{test}} \sigma_{\hat{Y}_{test}}}\right)^2 ; 0 \leq CoP \leq 1 \tag{5.7}$$

With a determined CoP, an ideal metamodel can be found. By adjusting the significance quantile from 99 percent to a set minimal value, each meta-model is explored for all potential significance. Following that, a polynomial regression is created, and the coefficients of significance (CoI) for each variable are obtained using Equation 5.8.

$$CoI_{Y,X_i} = R^2_{Y,X} - R^2_{Y,X\sim i} \tag{5.8}$$

Where $R^2_{Y,X}$ is the CoD of the full model, which includes all terms of the variables in *X*, and $R^2_{Y,X\sim i}$ is the CoD of the reduced model, which excludes all linear, quadratic, and interaction terms from X_i. The CoI_{Y,X_i} threshold is adjusted from 1% to a specific value. The meta-model is constructed using the CoI of each variable, and the coefficient of prognosis is calculated. From the maximal CoP configuration, the best meta-model is picked. The training data set is used to build the meta-model, whilst the test data set is utilized to calculate the CoP. For the correlations for the significance filter and the regression for the importance filters, on the other hand, a merge data set from training and test data is employed. If no extra test data set is available, the initial data set is split into training and test data in such a way that the response ranges in each data set are represented as closely as possible to the complete data set.

5.5. Multi Objective Genetic Algorithm (MOGA)

Multi-Objectives Genetic Algorithm (MOGA) is one of many engineering optimization methods, a guided random search technique. It is appropriate for solving multi-objective optimization problems with the ability to explore various regions of the solution space. As a result, a diverse set of solutions with more variables that can be optimized at the same time can be found. The Pareto fronts are used to illustrate MOGA solutions. A Pareto optimal set is a collection of non-dominated solutions on the solutions frontier. With the Pareto optimum set, the values of the corresponding objective function in the objective space are referred to as the Pareto front. Traditional multi-objective problem-solving methods include random searches, dynamic programming, and gradient methods, whereas modern heuristic methods include cognitive paradigms such as artificial neural networks, simulated annealing, and Lagrangian approaches. Some of these methods are capable of locating the best solution, but they have a tendency to take longer to converge, necessitating a significant amount of computing time. Thus, a MOGA approach based on the natural biological evaluation principle will be used to address this type of problem (Zolkapar 2020).

In general, engineering design issues necessitate the simultaneous optimization of many objectives as well as a set of constraints. Unlike single-objective optimization problems, the Pareto optimum set is a collection of points. The concept of Pareto dominance is used to compare solutions to one another. The following is an example of a multi-criteria optimization problem:

$$f_i(x)_i \qquad i=1\ldots,N \tag{5.9}$$

Subject to constrain,

$$g_j(x) = 0 \qquad j= 1,\ldots, M \tag{5.10}$$

$$h_k(x) \leq 0 \qquad k= 1,\ldots,M \tag{5.11}$$

where the objective functions, equality, and inequality constraints are f_i, g_j, and h_k, respectively. x is an n-dimensional vector, and N is the number of objective functions (Lee 2012).

Genetic Algorithms (GA), a subcategory of stochastic search methods, are search algorithms that are based on natural selection and genetics. In GAs, genes and chromosomes are the most important components. A chromosome is a gene strand. Genes are the variables that should be optimized in a real-world problem, and a chromosome is the solution to the problem. Genetic algorithms look for the best solution among chromosomal populations. They have the following benefits over other optimization techniques: Because they use probabilistic selection, they can handle multiple designs at once and temporarily accept less-than-ideal solutions. As a result, it is feasible to break free from the confines of a local minimum design zone.

Due of the ease space mapping of design variables into genetic strings to construct chromosomes, genetic algorithms are helpful tools for solving discrete issues. They use a population of potential solutions to do a multi-directional search. As a result, they execute crossover and mutation to present alternate solutions even if the optimal solution is not acceptable due to issues that were ignored from the optimization formulation. As a result, GA is well suited for the design and optimization of laminated composite structures with non-linear functions of plies, ply thicknesses, and orientation angles.

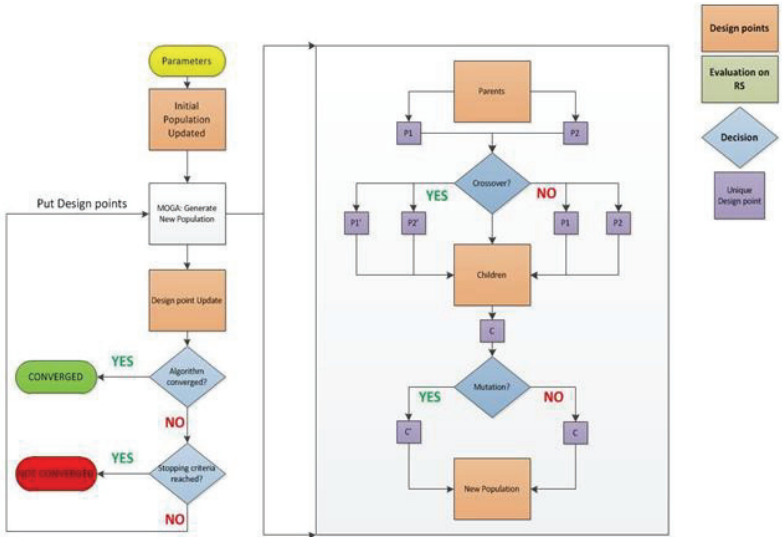

Figure 5.3 Processing steps of MOGA (Source: ANSYS 2020)

Multi-Objective Genetic Algorithms (MOGA) are a type of Genetic Algorithm that can do multiobjective optimization. MOGA is a controlled elitism variant of the popular

Nondominated Sorted Genetic Algorithm-II (NSGA-II). Figure 5 depicts the processing steps of the multiobjective genetic algorithm (MOGA). After creating the initial population at random, fitness function evaluation, selection, crossover, and mutation are carried out. The concept of elitism is established in order to find the best parents for the reproduction of children. The algorithm returns to the initial population if the criteria are not met (Beylergil, 2020).

5.6. Nondominated Sorted Genetic Algorithm-II (NSGA-II)

Nondominated Sorted Genetic Algorithm-II (NSGA-II) is a prominent multi-objective optimization technique that has three distinct features: a fast non-dominated sorting strategy, a quick crowded distance estimation procedure, and a simple crowded comparison operator (Deb 2002).

The NSGA-II algorithm is a multi-objective evolutionary algorithm develop by Deb et al (Deb 2002). The algorithm was built by fixing the flaws in Srinivas and Deb's NSGA algorithm (Srinivas 1995). The dominance grading and clustering distance calculation techniques are used in addition to the steps of the GA. NSGAII has a wide range of applications in the literature due to its low computational complexity, speed, and exclusivity.

In addition to engineering problems, the NSGA-II algorithm has been used to find the Pareto efficient cluster in a variety of situations, including worker assignment, project management decision alternatives, supply chain distribution, multi-period stock control, and determining the proper placement in wireless sensor networks. The decision makers are given with non-dominated points on the Pareto efficient set as solution possibilities. A fast non-pressurable sorting technique, stacking distance assignment, and a main loop make up the NSGA-II algorithm (Durmaz 20017).

In this study, the best angle alignments were tried to be optimized by using the evolutionary strategy of the genetic algorithm with the ANSYS Optislang interface program in order to find the optimum stacking sequence of the glass epoxy material in the experimental FML hybrid composite beam made in the reference article. Furthermore, the optimum material and angle alignment for two different material kinds are proposed with optimization utilizing a multi-objective genetic algorithm.

CHAPTER 6

RESULTS AND DISCUSSION

6.1. Problem Definition

Structural optimization is a phase of the structural design process that tries to systematically improve the structural performance of components and mechanical systems. In computer-aided engineering (CAE) designs, structural optimization has recently garnered a lot of attention. One of the reasons for quick development is to aid in the solution of engineering problems involving a large number of difficult mathematical equations as well as dependable analysis capability.

The finite element method (FEM) is the most extensively utilized solver approach in CAE designs. The FEM is a numerical procedure that breaks large geometric structures into very small elements that cannot be solved manually or using other traditional methods. However, several iterations with a trial-and-error method are required to arrive at the final design in FEM solutions. Although this 48 fits the design requirements successfully, it may not be the ideal answer for the final solution. Many analytical solution approaches were developed as computer technology advanced, allowing for more efficient solutions in less time than the trial-and-error approach. One of the ways that provide the optimum answer in line with this procedure is structural optimization methods, which have become increasingly popular in engineering research in recent years. The fundamental goal of these strategies is to discover a design that can be manufactured with the least amount of material and at the lowest cost while still offering the best performance. Structural design can be completed faster and at a lower cost using structural optimization methods rather than physical production in a virtual environment.

In this thesis, the buckling load capacity of a hybrid composite beam with fiber meatal laminate (FML) used in aircraft wing and fuselage parts was investigated. The optimum design of the anti-buckling behavior of the hybrid composite beam, which is subjected to in-plane compression load, fixed on both sides with a simple support, was investigated by genetic algorithm (GA) based on the Tsai-Wu fracture criterion. The robust design of composite hybrid laminates was aimed to be developed using a design

optimization process based on GAs and the finite element method. A Multi-Objective Evolutionary Algorithm (MOGA) was used to optimize the design of a hybrid composite beam subjected to buckling force. Design variables include to ply material and angle orientations. The purpose of the objective function is to reduce the hybrid composites Equivalent Stress while increasing critical buckling load. The design constraint was Tsai-Wu failure index.

Prior to obtaining the optimum designs of FML composite beam, verification of FEM numerical model, buckling load factor has been carried out using specific results from the study by Banat(2016) in the literature. The critical buckling load(P_{cr}) has been used as an objective function in optimization. Banat performed by determination of the buckling load capacity of a composite beam under compressive loads is critical for the design of the composite structures because the buckling could yield a premature failure of the structure. In the reference article, studies were carried out to investigate thin-walled channel section columns (C beams) produced by the autoclave. The buckling and post-buckling behavior of thin-walled Fiber Metal Laminate (FML) profiles subjected to axial loading is discussed in the Banat (2016).

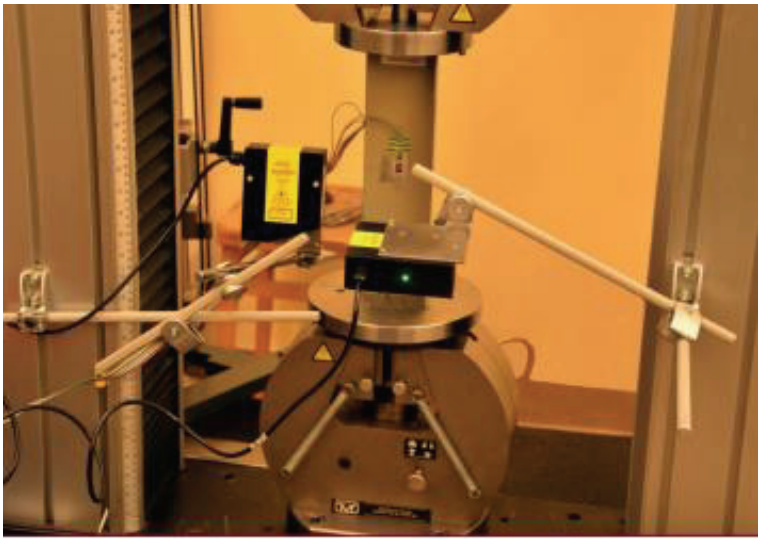

Figure 6.1. Tested C beam FML profile in the laboratory stand
(Source: Banat et. al. 2016)

Various 3/2-layer stackings were investigated and subjected to axial compression in buckling experiments depending on fibre alignment. Experiments were conducted to determine the buckling load and equilibrium routes in the buckling and post-buckling

states. The outcomes of extensive experimental investigations were compared to FML panel/columns modeling in FEA and analytically analyzed results. In conducted experiments (see Figure 6.1) the careful design of simply support boundary conditions of loaded edges of thin-walled columns is examined (Banat et. al. 2016).

In the FML beam studied in the article, the metallic layer is made of aluminum alloy 2024-T3, and the composite plies are made of glass-epoxy unidirectional fiber reinforced prepreg TVR 380 M12 with a 26 percent R-glass content. Material properties are given in Table 6.1.

Table 6.1 Material properties for aluminum and glass fiber

(Source: Banat et. al. 2016)

TVR 380 M12/26%/R-glass	**[GPa]**
E_1	46.43
E_2	14.92
E_3	14.92
G_{12}	5.233
G_{23}	3.57
G_{13}	5.233
ν_{12}	0.269
ν_{23}	0.4
ν_{13}	0.269
Al 2024-T3	**[GPa]**
E	72
ν	0.33
G	27
$R_{0.2}$	0.35
E_{tang}	0.72

The nominal volume fraction of the fibre in prepreg is around 60%, whereas the thickness of a single layer for aluminum and prepreg is 0.3 mm and 0.26 mm, respectively. Four different stacking sequences of FML have been considered in Banat's study (2016). In this study Al/0/90/Al/90/0/Al stacking sequences of FML have been studied for verification.

The composite beam under consideration has a channel section profiles with a length of is 300 mm. The web of the column is 80 mm wide, and the flanges are 40 mm wide. The web and flange junction's corner radius is 1.75 mm. Dimensions of considered C Beam section of FML is shown in Figure 6.2.

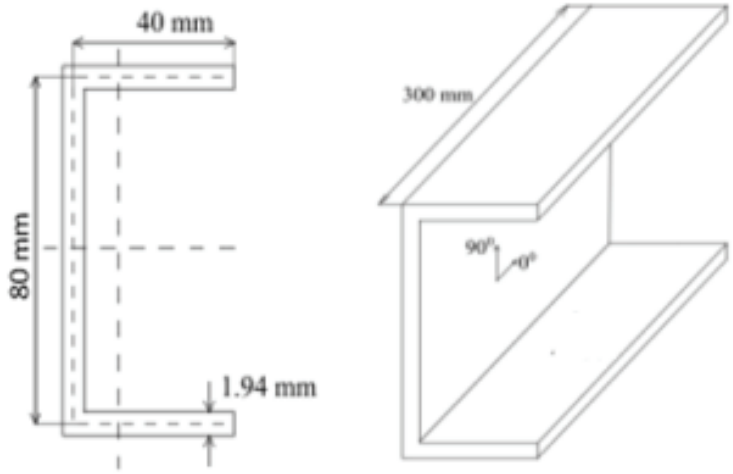

Figure 6.2. Dimensions of considered C Beam section FML column

The buckling analyses were carried out using the commercial ANSYS 2020 finite element software. First, the C beam defined in Figure 6.2 were drawn in the Spaceclaim program (see in Figure 6.3). The Spaceclaim program was developed as an alternative to the Design Modeler drawing program developed by ANSYS. Spaceclaim, which has a faster interface and simpler use, can easily perform geometry cleaning operations, which are necessary before analysis, as well as drawing tools. In order to create the geometry, a rectangle without a long side of 40x80 mm was drawn. For the corners, a fillet was made at R1.75 mm. Then the drawing was extended by 300 mm using the Pull command. In this way, the face element to be used is prepared in the Spaceclaim interface.

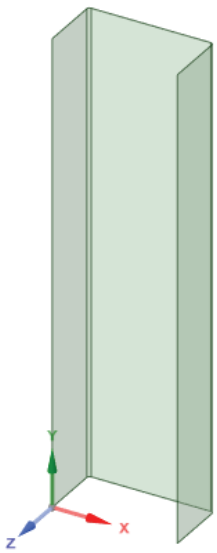

Figure 6.3. Image of face geometry in Spaceclaim program

A face element was used to speed up the analysis. In this way, a consideriable improvement was achieved in the solution time as a result of optimization. The thickness of the beam will be given together with the mesh structure. As it is seen in Figure 6.4, the mesh structure is uniform. Shell 181 (2D) elements were used to create a mesh structure of the composite beam. In total, 50100 Shell 181 elements and 50568 nodes were used for the 2D finite element model of the composite beam.

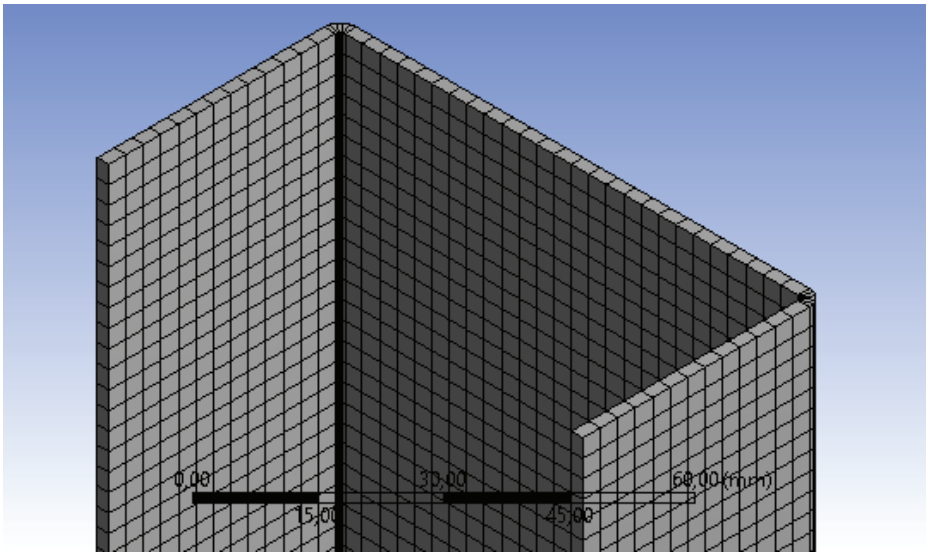

Figure 6.4. Image of mesh geometry for C beam

The SHELL181 element is four-node element having six degrees of freedom at each node: x, y, and z translations, as well as rotations around the x, y, and z-axes. (The element has only translational degrees of freedom if the membrane option is chosen.) In mesh generation, the degenerate triangular option should only be utilized as filler pieces. SHELL181 is ideal for nonlinear linear, big rotation, and/or large strain applications. Nonlinear analyses take into consideration changes in shell thickness. Both complete and limited integration techniques are supported in the element domain. SHELL181 accounts for distributed pressure follower (load stiffness) effects (ANSYS 2020).

As it is seen in Figure 6.5, the 3/2 arrangement with symmetrical lay-ups with regard to the wall midplane was examined for all FML profiles. '3' denotes three metallic layers, whereas '2' denotes two doubled embedded composite layers made up of two unidirectional GFRP prepregs (Banat et. al. 2016).

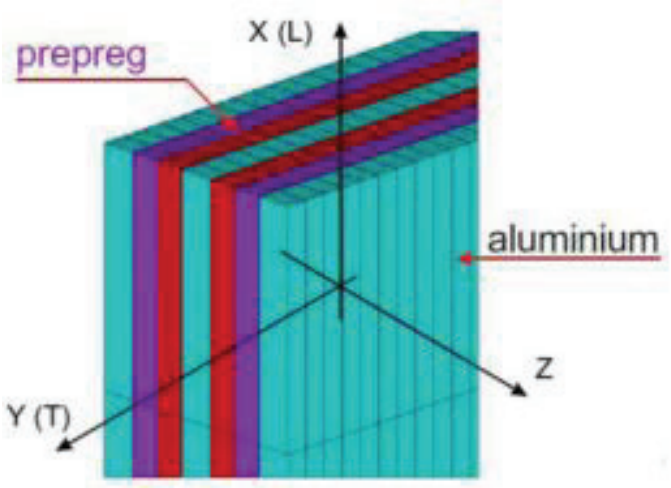

Figure 6.5. FML 3/2 specific lay-up configuration
(Source: Banat et. al. 2016)

The ANSYS ACP module is a module that contains all the requirements for the design of composite structures. By making fabrics from previously defined materials in this module, properties such as thickness and price can be entered. The thickness of the aluminum part is 0.3 mm and the glass fiber is 0.26 mm. Then Rosette was assigned to determine the fiber laying direction. As seen in Figure 6.6, Al/0/90/Al/90/0/Al (FML 3/2) hybrid composite has been successfully obtained.

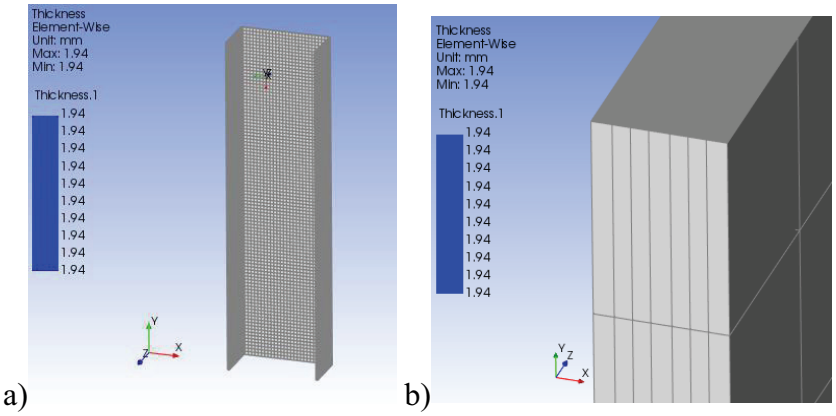

a) b)

Figure 6.6. a),b) Image of hybrid composite for 7 layers made with ACP-Pre modul in ANSYS

Simply supported conditions prevent lateral displacement of the loaded edges, can be seen Figure 6.7. The experiments were primarily focused on a simple FML thin-walled specimen test of complex plate structure. Three preloading compressions of up to 5 kN were performed before to the buckling test series. They increased specimen seating and

compression uniformity, reducing the risk of axial backslash. The load was steadily raised at a rate of 1 mm/min until it reached 1.5 times the FEM buckling load prediction (Banat et. al. 2016).

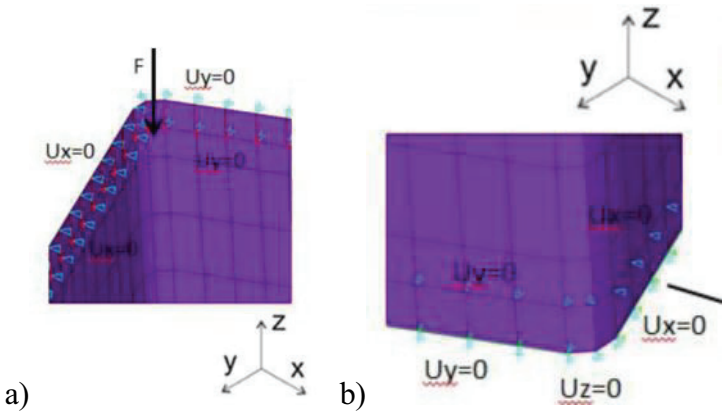

Figure 6.7. FEM model for a) the part that exerts the force on the beam, b) fixed part of the beam (Source: Banat et. al. 2016)

In the present study, displacement constraints were used to describe boundary conditions that corresponded to those assumed in the experiment and in the analytical approach that simply supported type. Lateral displacements were limited perpendicular to the profile walls along the upper and lower edges (displacements u_x=0 and u_y=0 in Fig. 6.8). Axial displacements were also limited at the bottom margins (u_z=0). A consistent nodal force distribution at the upper edge was used to approximate uniform compression of the profile. Additional coupling constraints (u_n= const) were added to ensure that the column edges were rectilinear. As a result of all of these displacement limits, boundary conditions suitable for the reference study are given.

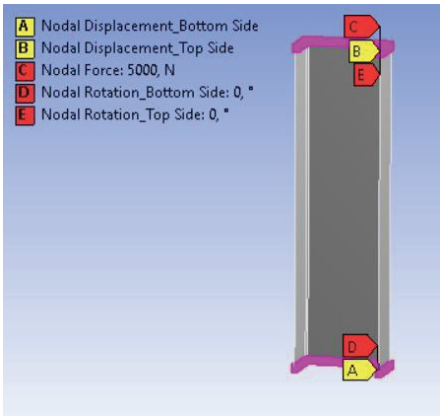

Figure 6.8. Boundary condition in Static Structure

After constructing the FML hybrit beam, linear buckling analysis was performed to determine the critical buckling load and the corresponding buckling mode shapes. The FEM was used to simulate the buckling behavior of open cross-section profiles subjected to axial compression using the commercial software program ANSYS. As can be seen in Figure 6.9 and Table 6.2, the results of the present study and the Banat's FEM study are very close to each other.

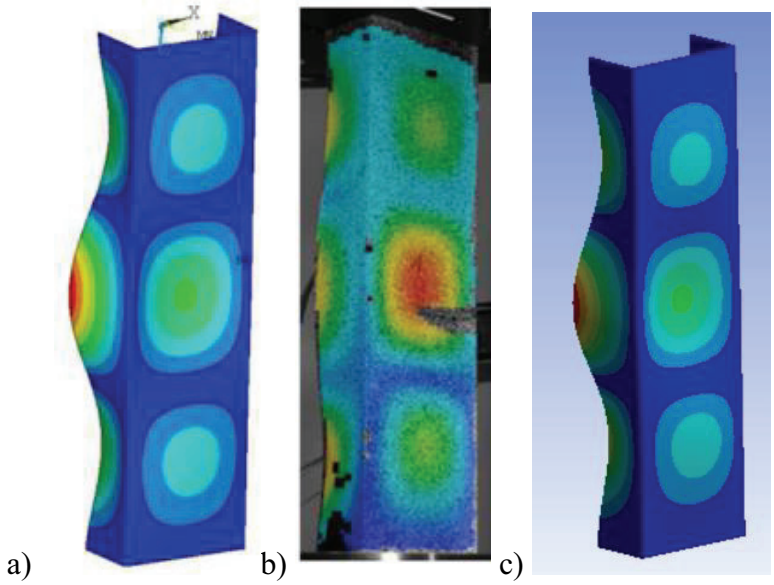

a) b) c)

Figure 6.9. Buckling modes comparison for C beam (a) FEM model
(b) visualization of the experiment (Source: Banat et. al. 2016)
(c) FEM analysis of the present study

Table 6.2 Critical load (P_{cr}) comparison for C beam

Sequence of Lay-up	P_{cr} Experiment [Banat] (kN)	P_{cr} - FEM[Banat] (kN)	P_{cr} - FEM[Present] (kN)
Al/0/90/Al/90/0/Al	31.434	30.189	29,309

In Banat's study (2016), there is a 4% difference between the experimental and FEM results. In the present study, there is less than 3% difference between FEM studies. The reason for the difference in the FEM studies is that the number of elements and nodes is not clearly specified in the reference study. A closer mesh and number of nodes will reduce the difference between the results.

The post-buckling analysis, which is the continuation of the validation study of the analysis was done. The solution in the post-buckling region until fracture, nonlinear

analysis of structure stability was necessary. Thus, the initial local mode shape produced in the context of linear buckling analysis was projected onto the finite element model's nodal mesh to form the imperfect walls of the considered beam. First, in ANSYS Mechanical Structure, instead of the force at the boundary conditions mentioned earlier, a displacement of 5 mm is defined. Then, the large deflection tool has been activated. In analysis, the stabilization energy needs to be selected as constant and the scale factor was taken 0.01 as in reference study. Table 6.3 shows that post-buckling result have good agreement with the Banat's result.

Table 6.3 Post buckling behavior force comparison for C beam (Al/0/90/Al/90/0/Al)

Axial Force	Banat result [kN]	Present Study [kN]
In 5 mm deflection	46	46.092

After successfully validating the analysis in terms of buckling using FEM, stacking sequence design optimization has been carried out for FML beam.

6.2. Optimization Results

Engineering's main concerns is the improvement of existing designs and the creation of optimal new ideas. Changes based on experience, intuition, or conjecture are traditionally used to achieve this. These procedures are inefficient, costly, and frequently deceptive. Many of today's engineering analysis cycles are extremely sophisticated as a result of the introduction of virtual prototyping. As a result, typical trial and error methods are ineffective in achieving intended results. Virtual prototyping is a multifaceted process. This fact adds to the difficulty. As a result, it's expected that a growing number of disciplines dealing with complicated (physical) phenomena will be required to participate in the design process. This multidisciplinary approach necessitates assessing many scenarios simultaneously while balancing multiple and frequently contradictory aims. As a result, a modern engineering strategy must use all available know-how in order to develop or construct designs.

The stresses that arise in the structure are much below those required to produce collapse in the material of which the structure is made, buckling can occur. Further

loading may result in severe and somewhat unanticipated deformations, potentially resulting in the member's load-carrying ability being completely lost. The member will continue to support the load that caused it to buckle if the deformations that occur after buckling do not cause it to completely collapse (Chun 2011).

Together with the use of fiber-reinforced composite materials, material design can be integrated into the structural design as an additional dimension Designers, materials scientists and structural engineers will benefit from the interaction of fiber, resin and fiber-resin interface in composite materials. Micromechanics, the current discipline that studies structural material interactions, is especially important for advanced composite analysis.

A complicated laminate design problem is the design of a laminate for strength. The usage of unidirectional or 45° orientations can efficiently satisfy the design for basic loading circumstances such as pure uniaxial or shear stresses. However, a laminate that must survive a wide range of stress situations and environments cannot be constructed efficiently with such design. Combinations of 0°, 45°, and 90° laminae can be used to create a simple design that is relatively efficient. On the other hand, computerized procedures, attain the highest levels of efficiency. For this reason, it is of great importance to carry out optimization studies in order to achieve the best result. (Chun 2011).

In this study, in order to find the optimum stacking sequences of the glass epoxy material in the FML hybrid composite beam the evolutionary strategy of the genetic algorithm with the ANSYS Optislang interface program has been used. Genetic algorithm is a hierarchical mathematical model whose purpose is to discover a solution by searching for the most suitable one in the population. By searching, the problem is approximated to a global optimum solution. The flow chart of the optimization in ANSYS Workbench is given in Figure 6.10. Material properties are entered in engineering data. Then, drawing C beam geometry in Spaceclaim. Meshing part making in the Model tool. After that, the ACP Pre-post was prepared for FML composite lamination. Glass epoxy ply orientations were chosen as input parameters for optimization. Boundary conditions were defined in the statics structure. Failure index and equivalent ztress was selected as the output parameter. The model and solution in the static structure were used with drag and drop in the eigenvalue buckling tool. In the model critical buckling load was selected as the output parameter. Using the parameter set, design points were created with MOP and preparations were made for optimization. Genetic algorithm tool was run according to the created design points.

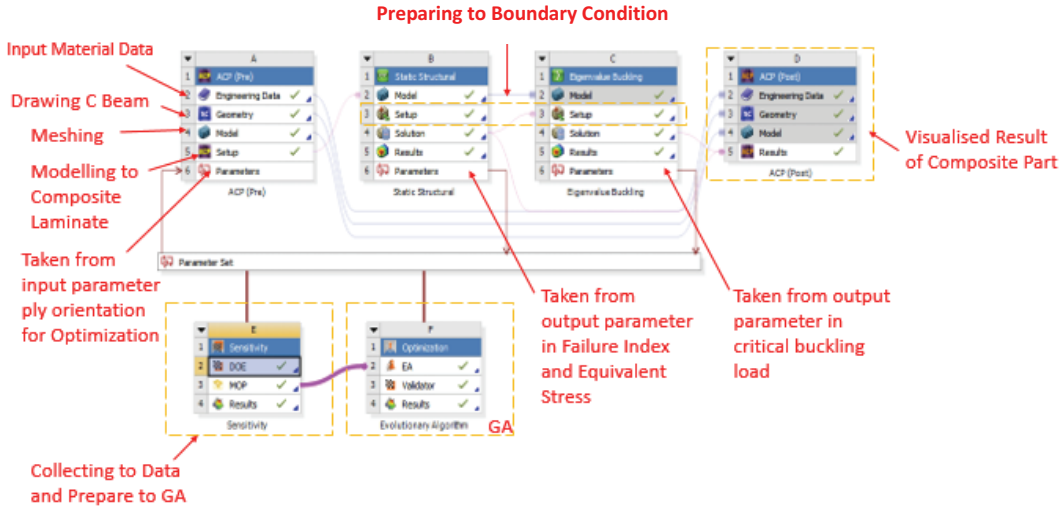

Figure 6.10. C beam optimization workflow

The ANSYS Workbench optiSLang Plugin enhances your product designs by merging ANSYS Workbench's advanced parametric modeling capabilities with optiSLang's methodologies. You can quickly drag and drop modules for sensitivity analysis, optimization, and robustness evaluation into a Workbench project to create an interactive process chain using the optiSLang toolbox (ANSYS 2020).

The sensitivity system creates a flow to begin a sensitivity study using ANSYS parameters that have been established. The following system components, Metamodel of Optimal Prognosis(MOP) and Design of Experiment(DoE), can be changed. The DoE dialog allows you to adjust specific algorithm settings, parameter properties, and criteria. Full factorial, axial, startpoints, central composite, d-optimal, d-optimal linear, LHS, LHS midpoint, A-LHS, and PMC are the sampling methods available. The central composite method is used in this thesis. The (MOP) algorithm settings can be changed in the property dialog. The optiSLang postprocessing will open to show the results of the MOP. Different subspaces of relevant input variables are examined with different meta-models to determine the MOP. As a result, a No Run Too Much technique is used to ensure the highest possible prognostic quality for the given number of design evaluations (ANSYS 2020). To see the statistics postprocessing of the DoE use the context menu of the DoE component and select "DoE Results".

ANSYS Optislang solver is used to improve the existing design and present new design proposals. As a first step, an optimization study was carried out for the orientation angles of the glass fibers in the existing FML hybrid composite beam. Composite plies are made of aluminum alloy 2024-T3 and its thickness is 0.3mm, and the glass-epoxy

unidirectional fiber-reinforced prepreg TVR 380 M12 with a 26 percent R-glass content and its thickness is 0.26 mm, and total weight is 250 g for FML beam.

A mathematical formula fitting to the data (input is stacking sequence, outputs are maximum buckling load, failure index), which is called a “response surface”. The parameters with significant affect on the outputs were determined from this formula, with which new response surfaces were created. Genetic aggregation metamodel was used to generate the response surface that is the most appropriate approach for each output compared to other metamodels. Figure 6.11 shows the predicted critical buckling (total deformation load multiplier) of the composite beam for different fiber orientations. Figure 6.11 shows the predicted critical buckling values (total deformation load multiplier) of the composite laminate for different fiber orientations. For the first ply of the composite laminate, critical buckling value has small differences decrease with the increase from 90° to 0°. For the second ply of the composite laminate, minimum critical buckling values were obtained for the composite laminates having 90° fiber orientation whereas the maximum critical buckling for 0° fiber orientation. This behavior was observed also for the sixth ply. On the other hand, in the fifth ply, the critical buckling value took its maximum value for 90° orientations, while these ply values were not affected by the angle orientation for the critical buckling load.

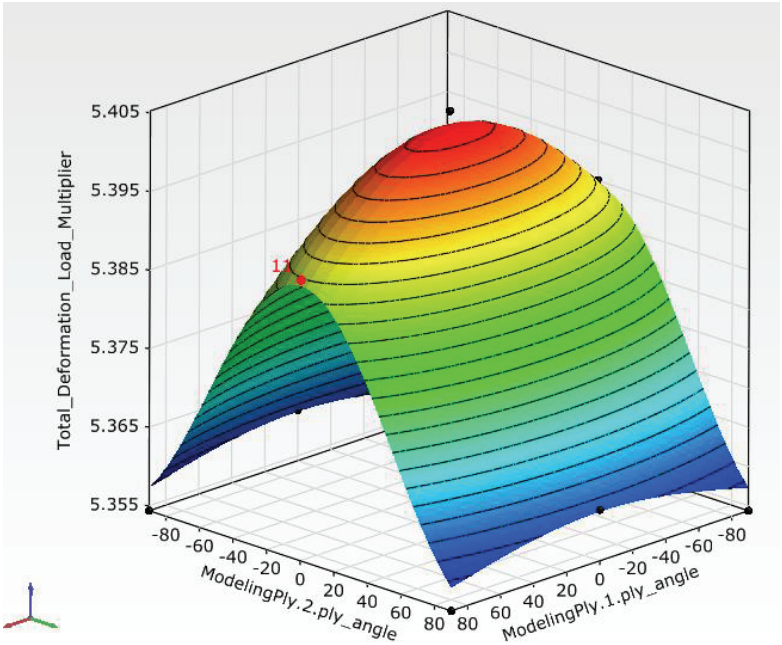

a)

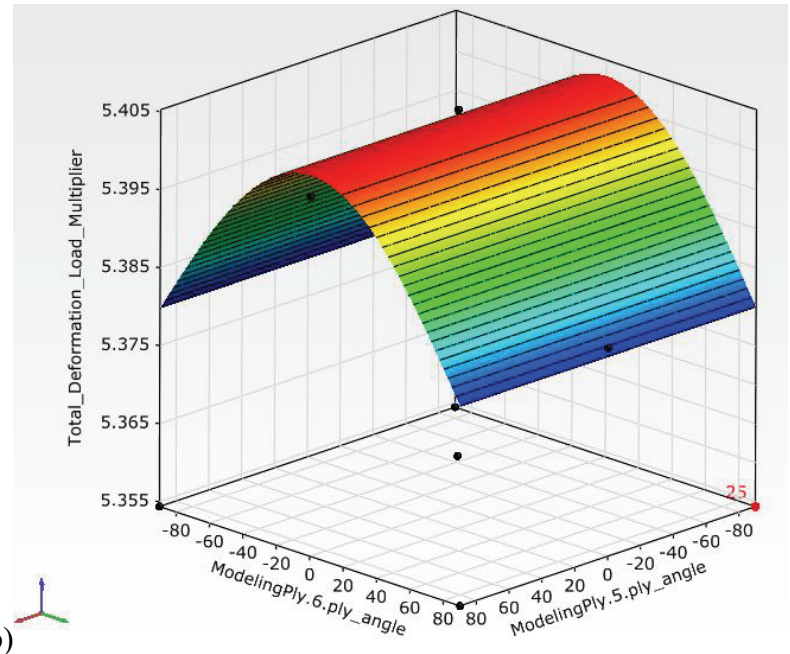

b)

Figure 6.11. The effect of fiber orientations a) the first and second plies, b) on the fifth and sixth plies for critical buckling

In Figure 6.12, the best result is shown to glass fiber stacking sequences for FML beam. The first and sixth layers' angle orientation -3° and -4° were obtained. Angle orientation for the second ply is -80° and the fifth ply is 90°. These results are consistent with the results obtained on the response surface. In terms of manufacturability, the first and second layers can be taken at 0°, and the number 2 layer can be taken at 100°. Thus, the optimum stacking sequences Al/-80/-3/Al/90/-4/Al were obtained.

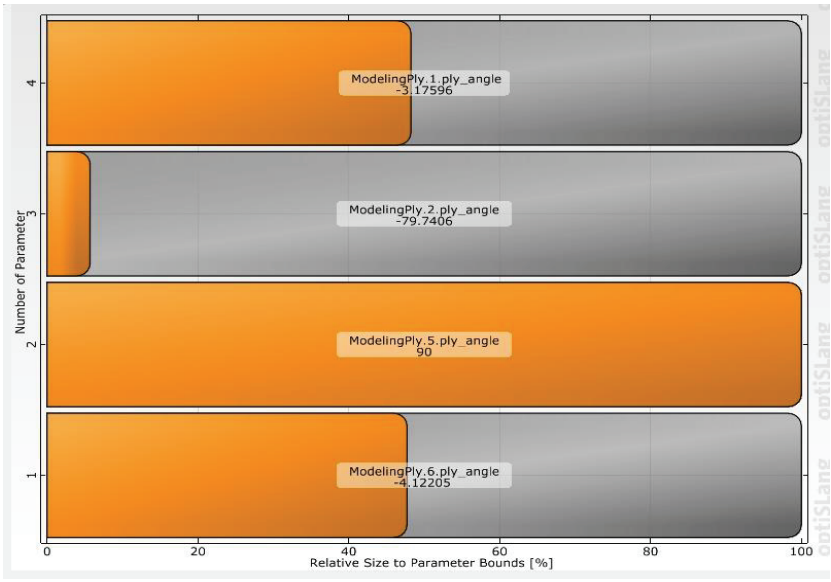

Figure 6.12. Optimum solution of stacking sequences for each ply

The Coefficient of Prognosis (CoP) quantifies the forecast quality of a meta-model (regression model) for the prognosis of a result value. Sensitivity measures depend on global CoP and the target CoP be 80% shall be reached (ANSYS 2020). Given in Figure 6.13, very reliable values have been achieved since our CoP value is 100%. Total CoP from MOP run was found 100% which was considered significant enough for the optimum parameter identification.

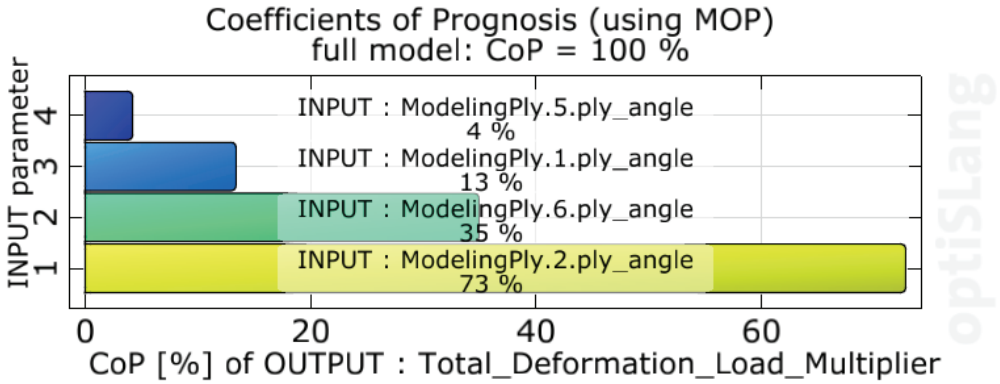

Figure 6.13. CoP value for each significant parameter.

Nature-inspired algorithms, such as the Genetic Algorithm (GA), are gaining traction in solving difficult engineering issues. It created 9900 design points according to the input parameters and successfully solved these created design points. Out of these design points, 781 were selected as a result. Given the optimum design results of the FML beam with the evolutionary strategy of the genetic algorithm. Output variable(critical buckling load anda Tsai-Wu failure index) results are seen in Figure 6.14. While the critical buckling gives 31,828 kN, the failure criteria is 0.03. Also, the Maximum Equivalent Stress is 52,398 Mpa.

Table 6.4 Comparison of critical buckling load

FEM Comparison	**Sequence of Lay-up**	**P_{cr} [kN]**
Banat Stuyd	Al/0/90/Al/90/0/Al	30.189
Presented Study	Al/-80/-3/Al/90/-4/Al	31.828

All output parameters have been improved. As seen in the table 6.4, the critical buckling load of the FML beam has been improved with the best stacking sequences

obtained with the optimization. It showed that the fold orientation of the glass fibers had an effect on the critical buckling load on the FML beam. The failure index gave very safe results. The reason for this is that aluminum has a great say against the compressive force in the FML hybrid composite for buckling behavior. The results have been shown that glass fiber ply orientation in the hybrid composite stacking sequences has an effect on the total buckling load value of the FML thin-walled beam under consideration.

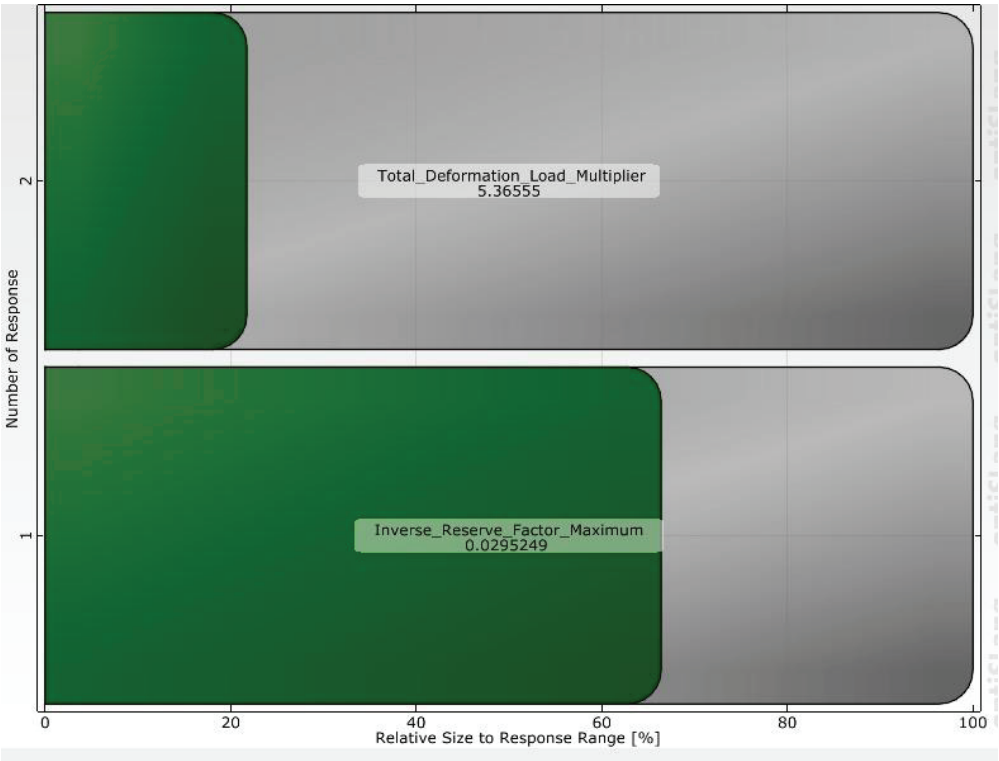

Figure 6.14. Response data for each output variable

The results have been shown that glass fiber in the hybrid composite stacking sequences has an impact on the total buckling load value of the FML thin-walled beam under consideration.

In order to improve the mechanical and buckling properties of the present hybrid composite beam, a new hybrid composite design was proposed. In proposed design, 8-layered composite with carbon fiber and glass fiber epoxy which is thickness of 0.25 mm each ply are used. Also, total weight is 213g proposed hybrid composite beam. Glass epoxy material is located in the middle layer (1 and 5) and carbon fiber in the other layers (See Figure 6.15) . The material properties are given in Table 6.5.

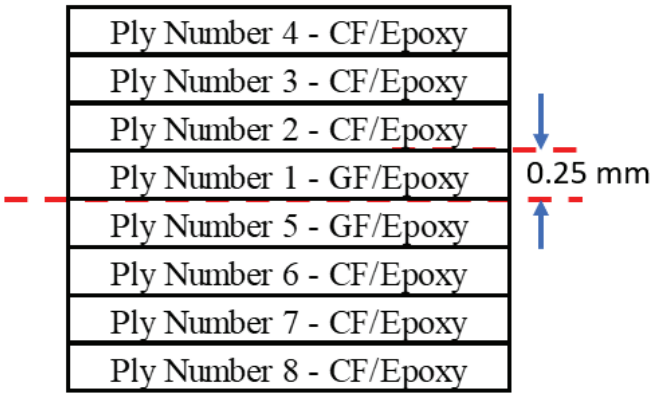

Figure 6.15. Ply orientation sequence in ANSYS ACP module

Table 6.5 Mechanical properties of unidirectional carbon and glass epoxy fibers (Source: Beylergil 2020).

Material [GPa]	**CF-EP**	**EG-EP**
E_1	123.34	45
E_2	7.78	10
E_3	7.78	10
G_{12}	5	5
G_{23}	3.08	3.846
G_{13}	5	5
ν_{12}	0.27	0.3
ν_{23}	0.4	0.4
ν_{13}	0.27	0.03

Same finite element procedure using again. In the optimization process, ANSYS Direct Optimization tool with Multi-Objective Genetic Algorithms (MOGA) is used. Multi-Objective Genetic Algorithm is a type of Genetic Algorithm that can do multi objective optimization. The operation steps mention take into account different objectives and constraints in order to discover the global best solution for the GA. The flow chart of the method used here is presented in Figure 6.16.

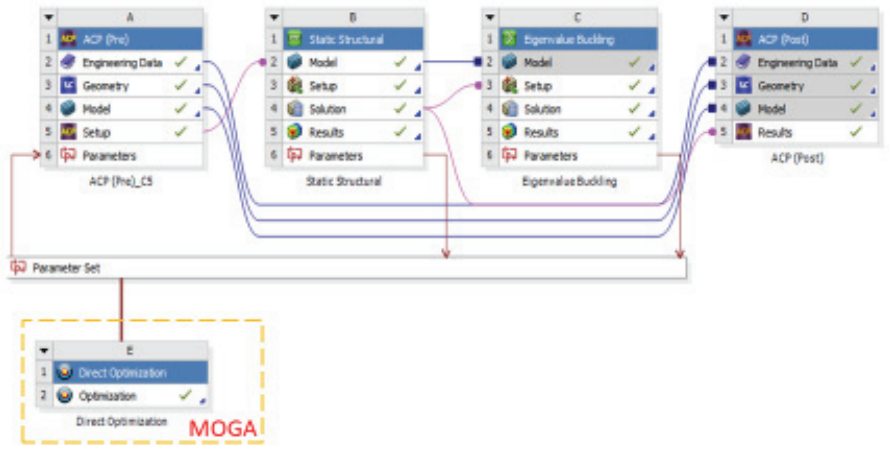

Figure 6.16. Optimization flow chart in ANSYS

Multi-Objective Genetic Algorithms are a type of Genetic Algorithm that can do multi objective optimization (MOGA). MOGA is a controlled elitism variant of the popular Nondominated Sorted Genetic Algorithm-II (NSGA-II). Figure 6.17 depicts the processing steps of the MOGA. The process steps of the finite element analysis part were mentioned in detail in the previous sections. The same process steps will be used in this analysis.

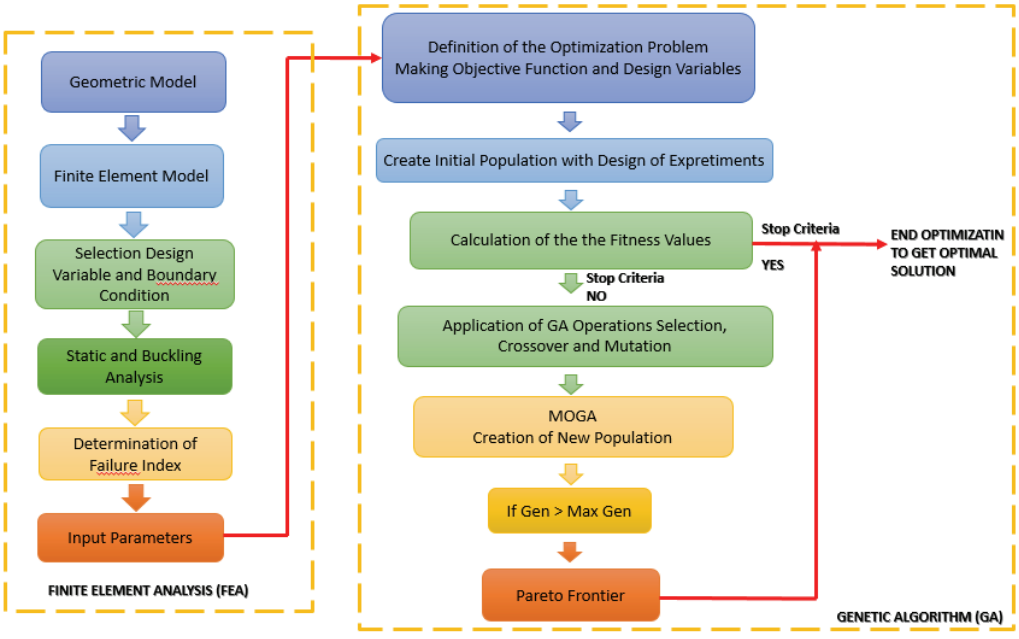

Figure 6.17. Operation steps with MOGA in present study

The operation steps mention take into account different objectives and constraints in order to discover the global best solution for the GA. After creating the initial

population at random, fitness function evaluation, selection, crossover, and mutation are carried out. The concept of elitism is established in order to find the best parents for the reproduction of children. The algorithm returns to the initial population if the criteria are not met. The mathematical formulation of the optimization problem is given below.

Objective function

- Maximize critical buckling load
- Minimize Equivalent Stress

Design variables

- Ply angles: $-90 \leq \theta_n \leq 90$; n = 1, 2,....,8
- Ply material: CF-EP and EG-EP

Constraints

- Tsai-Wu failure index FI ≤ 0.34

Objective function are maximize critical buckling load and minimize equivalent stress of the the hybrid composite beam. The minimal safety factor was chosen 3. The design constrain is each ply's maximum Tsai-Wu failure index should be less than 0.34. The target variability value is to maximize the current critical buckling load. Two design inputs considered are ply angle and ply material. Ply angle was determined between -90 and 90 degrees with 10 degrees of variability. Carbon and glass epoxy fibers were chosen as materials for all 8 fibers.

Direct Optimization was started after the finite element step was completed. The first step was to build an experimental design. A design of trials based on Central Composite Design (CCD) was set up, yielding 342 Design Points for the six-teen input design parameters. The output data at these 342 Design Points was then generated automatically. Generate 66 samples initially, 66 samples per iteration and find 3 candidates in a maximum of 6 iterations. The MOGA parameters utilized in this study are listed in Table 6.6. The MOGA was carried out with a total of 66 samples, with 66 samples each iteration.

Table 6.6 Used MOGA parameters

Crossover rate	0.98
Mutation rate	0.1
Pareto percentage (%)	70
Number of iterations	6
Pareto percentage	1.5195

The maximum permissible pareto percentage, which indicates the number of intended pareto points divided by the number of samples per iteration was 70%. The optimization is said to be converged when this 70% is obtained. For most optimization situations, this number is chosen between 0.55 and 0.75. To avoid premature convergence concerns, a high crossover rate of 98 percent was used, and a low mutation rate of 10% was chosen to prevent genetic algorithms from sliding into local maxima or minima.

The best design according to the optimization results are given in Table 6.7. When the stacking sequences design was examined, the plies were generally ±40/50 degrees according to the optimization results. It is natural for the analysis to converge in this way because as known in the literature, multiples of ±45° give better buckling strength. Glass fibers located on the 1th and 5st plies as the center of the layer, an angle of 80 and 90° was obtained. In long beams and panels, 90° plies assist in better stability than 0° plies. In addition, since the resistance to compression forces is high in composite materials, it is expected that the glass fiber converges to 90°.

Table 6.7 Best desing for optimization results

Ply Number	**Optimum Stacking Sequences**
1 - GF-Epoxy	80
2 - CF- Epoxy	-50
3 - CF- Epoxy	-50
4 - CF- Epoxy	50
5 - GF- Epoxy	90

(cont. on next page)

Table 6.7. (cont.)

6 - CF- Epoxy	45
7 - CF- Epoxy	-40
8 - CF- Epoxy	50
Critical Buckling Load (kN)	34.273
Tsai-Wu Failure Criteria	0.16
Maximum Equivalent Stress (MPa)	50.704

As seen from the Table 6.8 the critical buckling load factor for the beam obtained 34.273 kN. When it is compared with FML beam actually their beam geometrical dimension is nearly closed to each other. As you see that we obtained entirely composite beam construction gave us a good result. Additionally, when the optimum design is compared with the FML composite beam, a 15% weight reduction is achieved. We have verified study also by compared to equivalent stress is reduced. This is a preferred situation in the aviation sector.

Table 6.8. Comparison for C beam

	FML Beam[Banat]	**FML Beam**[Altıntaş]	**Proposed Beam**[Altıntaş]
Critical Buckling Load	29.309 kN	31.828 kN	34.273 kN
Weight	250 g	250 g	213 g
Maximum Equivalent Stress	57.548 MPa	52.398 MPa	50.704 MPa

Although the use of carbon fiber was thought to be expensive in terms of cost, a very advantageous design was obtained considering the mechanical advantages of carbon fiber as well as the cost of stock and the compatibility with glass fiber. The MOGA approach was found to be beneficial in improving the structural performance of a hybrid composite beam under compressive loads.

CHAPTER 7

CONCLUSION

In this thesis, the design of composite hybrid laminates (carbon/epoxy,glass/epoxy) having channel cross-section (C-shape) was improved using a design optimization process based on GA and the Finite Element Method. A multi-objective evolutionary algorithm (MOGA) was used to optimize the design of a hybrid composite beam that was subjected to a combined compressive load. Design variables include the ply material and lay-up orientations. The purpose of the objective function is to reduce equivalent stress while increasing critical buckling load. Design limitations are the Tsai-Wu failure index of the composite beam.

First, the buckling load was verified by the Finite Element Method (FEM) using the specific results given in previous studies in the literature.

Determination of the buckling load of the FML beam in different angle directions of the glass fiber material was investigated based on the data obtained in the reference study. The evolutionary strategy of the genetic algorithm was used to achieve the best stacking sequences. Design inputs were created in the ANSYS Optislang program. 25 new design points were created as fiber angle ($-90° \leq \theta_n \leq 90°$) with the Central Composite Design (CCD). With these design points, the new 9900 different design results regarding the given boundary conditions have been performed by using GA. A new optimization result was obtained according to the stacking sequences of the four glass epoxy fibers. Output parameters were determined according to the critical buckling load and Tsai-Wu failure index. The results show that although the presence of certain stacking sequences of glass fibers layers affects the profile response, aluminum has a significant effect on a critical load and Tsai-Wu failure index.

The existing design improved with a new optimization study to suggest different material and fiber angles. MOGA was used for the optimization of the design of a C beam composite laminate consisting of carbon and glass fiber/epoxy plies that were exposed to compressive load. Design factors include ply material (carbon fiber or epoxy glass fiber) and fiber orientations ($90° \leq \theta_n \leq 90°$). The aim of the objective function is to reduce equivalent stress while increasing critical buckling load. Design limitations are the Tsai-Wu failure index of the composite beam. ANSYS Workbench with the ACP module was

used to conduct the numerical analyses. Determination of the best stacking sequences according to the ply materials used with the Direct Optimization tool in ANSYS. In order to increase the structural performance of the composite beam under an axial compression load, the best stacking sequences were obtained with MOGA. Based on the CCD design of trials, 342 design points were created. The output data was then created automatically at these 342 design points. Initiating with 66 samples, it was found three candidates in a maximum of six iterations. Each ply's fiber orientation was modified from 90 to 90 degrees with a 10-degree increment. When the stacking sequences design was examined, the carbon fiber/epoxy were generally ±40/50 degrees according to the optimization results. The analysis converges in this way because as known in the literature, multiples of ±45° give better buckling strength. Glass fibers/epoxy were located in the center of the layer, an angle of 90° was obtained. In long beams and panels, 90° plies assist in better stability than 0° plies. In addition, since the resistance to compression load is high in composite materials, it is expected that the glass fiber converges to 90°.

Despite the use of an extra layer of the hybrid composite beam of the same thickness is reduced by 15% compared to the FML design. Although, the use of carbon fiber was thought to be expensive in terms of cost at first, a very advantageous design was obtained considering the mechanical advantages of carbon fiber as well as the cost of stock and the compatibility with glass fiber. The MOGA approach was found to be beneficial in improving the structural performance of a hybrid composite beam under compressive loads.

REFERENCES

Adali S., Lene F., Duvaut G., Chiaruttini V., 2003, Optimization of laminated composites subject to uncertain buckling loads, Composite Structures, 62, 261-269.

Ahmad, F., Choi H. S., Park M. K., 2014, A Review: Natural Fiber Composites Selection in View of Mechanical, Light Weight, and Economic Properties Macromolecular Materials and Engineering, 10-24.

ANSI/AISC, July 7, 2016, Specification for Structural Steel Buildings, An American National Standard, 360-16.

ANSYS Inc., 2020, ANSYS Release Notes Reference, Release 2020 R1.

Baba B. O., 2007, Buckling Behavior of Laminated Composite Plates , Journal of Reinforced Plastics and Composites, 26 (16), 1637–55.

Banat D., Kolakowski Z., R J Mania, 2016, Investigations of fml profile buckling and post-buckling behaviour under axial compression, Thin-Walled Structures, 107, 335–344.

Barbero E. J., 2013, Finite Element Analysis of Composite Materials Using ANSYS®, CRC Press.

Beylergil B., 2020, Multi-objective optimal design of hybrid composite laminates under eccentric loading, Alexandria Engineering Journal, Volume 59, Issue 6, Pages 4969-4983.

Chen Y., Wang Y., Wang H., 2020, Research Progress on Interlaminar Failure Behavior of Fiber Metal Laminates, Advances in Polymer Technology.

Chun M., Yung N., 2011, Airframe Structural Design Practical Design Information and Data on Aircraft Structures, Adaso & Adastra Engineering Center.

Clyne T. W., Hull D., 20019, An Introduction to Composite Materials, Cambridge University Press.

Deb, K., Pratap A., Agarwal S., Meyarivan T., 2002, A fast and elitist multiobjective genetic algorithm: NSGA-II Evolutionary Computation, IEEE Transactions on, 6, 182-197.

Deveci H. A., Aydin L., Artem H. S., 2016, Buckling Optimization of Composite Laminates Using a Hybrid Algorithm under Puck Failure Criterion Constraint, Journal of Reinforced Plastics and Composites, 35 (16), 1233–47.

Duong C. N. W., Chun H., 2016, Bonded Joints and Repairs to Composite Airframe Structures, Academic Press is an imprint of Elsevier.

Durmaz E. D., Şahin R., 2017, NSGA-II and goal programming approach for the multi-objective single row facility layout problem, Journal of The Faculty Of Engineering And Architecture Of Gazi University, vol 32, no 3, pp 941-955.

Erdal O., Sonmez F. O., 2005, Optimum design of composite laminates for maximum buckling load capacity using simulated annealing, Composite Structures, 71, 45-52.

Ever B., 2010, Introduction to Composite Materials Design, CRC Press.

Gurdal Z., Haftka R. T., Hajela P., 1999, Design and Optimization of Laminated Composite Materials, John Wiley & Sons, Inc.

Hoffman O., 1967, The brittle strength of orthotropic materials, Journal of Composite Materials, Vol 1, No 2, 200-206.

Irisarri F. X., Bassir D. H., Carrere N., Maire J. F., 2009, Multiobjective stacking sequence optimization for laminated composite structures, Composites Science and Technology, 69, 983-990.

Kamocka M., Mania R. J., 2015, Analytical and Experimental Determination of FML Stiffness and Strength Properties Mechanics and Mechanical Engineering, Vol 19, No 2, 141-159.

Karakaya Ş., Soykasap Ö., 2009, Buckling optimization of laminated composite plates using genetic algorithm and generalized pattern search algorithm, Struct Multidisc Optim, 39, 477-486.

Kaw, A. K., 2006, Mechanics of Composite Materials, Taylor & Francis Group, LLC.

Kim C. W., Lee J. S., 2005, Optimal design of laminated composite plates for maximum buckling load using genetic algorithm, Proceedings of the Institution of Mechanical Engineers, Part C: Journal of Mechanical Engineering Science, 219, 869-878.

Kolakowski Z., Kubiak T., 2005, Load-carrying capacity of thin-walled composite structures, Composite Structures, 67, 417–426.

Koza J. R., 1992, Genetic Programming: on the Programming of Computers by Means of Natural Selection, vol 1, MIT press.

Krenkel W., Reichert F., 2018, Design objectives and design philosophies, interphases and interfaces in fiber-reinforced CMCs, in Comprehensive Composite Materials II, RugglesWrenn, MB, editor Elsevier, 1–18.

Lee D. S., Morillo C., Bugeda G., Oller S., Onate E., 2012, Multilayered composite structure design optimisation using distributed/parallel multi-objective evolutionary algorithms, Compos Struct 94 (3), 1087–1096.

Liu B., Haftka R. T., Akgün M. A., Todoroki A., 2000, Permutation genetic algorithm for stacking sequence design of composite laminates, Comput Methods Appl Mech Engrg, 186, 357-372.

Lopez R. H., Luersen M. A., Cursi E. S., 2009, Optimization of laminated composites considering different failure criteria, Composites: Part B, 40, 731- 740.

Lupescu M. B., 2004, Fiber Reinforcements for Composite Materials, Editura Tehnica, Bucuresti.

Mallick P. K., 2007, Fiber-reinforced composites : materials, manufacturing, and design, Taylor & Francis Group, LLC.

Mania R. J., Kolakowski Z., Bienias J., Jakubczak P., Krzysztof M., 2015, Comparative study of FML profiles buckling and postbuckling behaviour under axial loading, Composite Structures, 134, 216–225.

Most T., Will J., 2008, Metamodel of Optimal Prognosis-an automatic approach for variable reduction and optimal metamodel selection, Proc Weimarer Optimierungs- und Stochastiktage, 5, 20–21.

Naik G. N., Gopalakrishnan S., Ganguli R., 2008, Design optimization of composites using genetic algorithms and failure mechanism based failure criterion, Composite Structures, 83, 354–367.

Pai N., Kaw A., Weng M., 2003, Optimization of laminate stacking sequence for failure load maximization using Tabu search, Composites: Part B, 34, 405- 413.

Pelletier J. L., Vel S. S., 2006, Multi-objective optimization of fiber reinforced composite laminates for strength, stiffness and minimal mass, Computers and Structures, 84, 2065–2080.

Puck A., Schürmann H., 2002, Failure analysis of FRP laminates by means of physically based phenomenological models, Composites Science and Technology, 62, 1633–1662.

Rao S., 2019, Engineering Optimization: Theory and Practice John Wiley & Sons.

Riche L. R., Haftka R. T., 1995, Improved Genetic Algorithm For Minimum Thickness Composite Laminate Design, Composites Engineering, 5(2), 143- 161.

Shahnewaz M., Alam M. S., 2020, Genetic algorithm for predicting shear strength of steel fiber reinforced concrete beam with parameter identification and sensitivity analysis, Journal of Building Engineering, 29, 101-205.

Soltani P., Keikhosravy M., Oskouei R. H., Soutis C., 2011, Studying the Tensile Behaviour of GLARE Laminates: A Finite Element Modelling Approach, Appl Compos Mater, 18, 271–282.

Soremekun. G., Gürdal Z., Haftka R. T., Watson L. T., 2001, Composite laminate design optimization by genetic algorithm with generalized elitist selection, Computers and Structures, 79, 131-143.

Soykasap Ö., Karakaya Ş., 2007, Structural Optimization Of Laminated Composite Plates For Maximum Buckling Load Capacity Using Genetic Algorithm Key Engineering Materials 348-349: p 725-728.

Soykasap Ö., Karakaya Ş., 2007, Structural Optimization of Laminated Composite Plates for Maximum Buckling Load Capacity Using Genetic Algorithm, Key Engineering Materials, 348-349, 725-728.

Spallino R., Thierauf G., 2000, Thermal buckling optimization of composite laminates by evolution strategies, Computers and Structures, 78, 691-697 73.

Srinivas N., Deb K., 1995, Multiobjective optimization using nondominated sorting in genetic algorithms, Evol Comput , 2 (3), 221-248.

Tanaka F., Okabe F., 2018, Historical review of processing, microstructures, and mechanical properties of PAN-based carbon fibers, in Comprehensive Composite Materials II, Gdoutos, EE, editor Elsevier, 66–85.

Topal U., Uzman Ü., 2008, Thermal buckling load optimization of laminated composite plates, Thin-Walled Structures, 46, 667-675.

Walker M., Reiss T., Adali S., 1997, Optimal design of symmetrically laminated plates for minimum deflection and weight, Composite Structures, 39(3-4), 337-346.

Walker M., Smith R. E., 2003, A technique for the multi-objective optimization of laminated composite structures using genetic algorithms and finite element analysis, Composite Structures, 62, 123-128.

Zhang J., Bisagni C., 2021, Buckling-driven mechanisms for twisting control in adaptive composite wings, Aerospace Science and Technology, 118.

Zolpakar N. A., Lodhi S. S., Pathak S., Sharma M. A., 2020, Application of Multi - Objective Genetic Algorithm (MOGA) Optimization in Machining Processes In: Gupta K , Gupta M (eds) Optimization of Manufacturing Processes Springer Series in Advanced Manufacturing Springer.